8-2016

Photoluminescence Measurement on Low-temperature Metal Modulation Epitaxy Grown GaN

Yang Wu
University of Arkansas, Fayetteville

Photoluminescence Measurement on Low-temperature Metal Modulation Epitaxy Grown GaN

A thesis submitted in partial fulfillment
of the requirements for the degree of
Master of Science in Physics

By

Yang Wu
University of TianJin University
Bachelor of Science in Optoelectronics, 2011

August 2016
University of Arkansas

This thesis is approved for recommendation to the Graduate Council.

Dr. Gregory J. Salamo
Thesis Director

Dr. Hugh O. H. Churchill
Committee Member

Dr. Morgan E. Ware
Committee Member

Dr. Reeta Vyas
Committee Member

Abstract

A low-temperature photoluminescence (PL) study was conducted on low-temperature metal modulation epitaxy (MME) grown GaN. By comparing the PL signal from high temperature grown GaN buffer layers, and MME grown cap layers on top of the buffer layers, it was found that MME grown GaN cap has a significantly greater defect-related emission. The band edge PL from MME grown GaN found to be 3.51eV at low temperature. The binding energy of the exciton in GaN is determined to be 21meV through temperature dependence analysis. A PL peak at 3.29eV was found in the luminescence of the MME grown cap layer, which was not observed before. The thermal activation energy of this peak is determined to be 33meV. Emission at this energy in previous GaN material has been shown to be the result of stacking faults. We believe this peak in the MME GaN is also the result of stacking faults. In droplets were used as a surfactant to improve the quality of MME grown GaN. By comparing the PL signal from samples with and without In surfactant, it was found the 3.29eV PL peak disappears with the use of In droplet, which indicates the surfactant effect of In droplet has reduced the formation of these stacking faults.

Acknowledgement:

I own a deep sense of gratitude to my advisor, Dr. Salamo, who leads me through the research, encourages me when I feel frustrated and depressed about the research outcome. I've benefited from his attitude to science, which inspires me to explore more, and to earn the respect from people with my best effort. Without his help, I won't be able to accomplish this work.

I also own a deep sense of gratitude to Dr. Morgan, who taught me to do the experiment and always support me when I run into any problem. No matter it's a problem with equipment, analysis or writing. He was acting as my hero through the time. I've benefited a lot from his wide knowledge of this field and his accompany whenever I got a problem.

My special thanks go to Ann Hu, Chen Li and Yusuke Hirono, who are also students in the same research group with me. There are many times when I have to work late, it's their accompany that makes me feel the experience of doing experiment late in the building is kind of a cool thing to do. It's the discussion with them that opens up my mind to think about the problem in a new perspective. It's my honor to have the friendship and accompany of those smart and interesting people.

Table of Contents

Chapter 1 Introduction

1.1 Problem

1.1.1History of GaN

GaN is a type of material that doesn't exist in nature. Since 1930[1], Johnson et al synthesized GaN for the first time through the reaction of halides of gallium with ammonia gas, GaN had its debut in the people's eye. In 1969, people starts to deposit GaN film on sapphire substrates using metal-organic chemical vapour deposition (MOCVD) method [2]. This invention encouraged the true interest to develop the technique of GaN growth, as this material was expected to be as successful as its counterparts in group III-V semiconductors in short wavelength range because of its wide band gap. However, in order to apply GaN for electrical devices, the quality of the material still needs to be improved. Back at that time, there were two major problems of GaN material that need to be solved:

- 1 proper substrate

Due to the lack of natural GaN substrate, people had to grow GaN on a sapphire substrate which has a big lattice mismatch with the GaN lattice. The quality of GaN epitaxial film was greatly affected by the substrate, while the quality of substrate in the early days was so unsatisfying that a lot of defects were generated in the material.

- 2 p-type doping

The GaN material made at that time was naturally n-type doped. The popular explanation of the cause is the intrinsic Ga vacancy defect which forms a donor level in the material.

If people want to make p-n junction with GaN material, p-type doped GaN had to be created.

From 1969 to date, a lot of progress has been made on the growth of GaN. In 1983, Yoshida tried to grow GaN on an AlN buffer layer and found the quality was greatly improved by doing that. [3] Nakamura gains the same success by using a low-temperature GaN buffer layer [4]. After the quality of the GaN crystal was improved, the focus was on P-type doping. In 1989, Amano accidently found p-type doping using Mg in GaN can be activated by the radiation of a low energy electron beam.[5] The p-type carrier density was greatly improved after the radiation. After that, people found Fe doping in GaN results in p-type material also [6].

Since high-quality p-type GaN appeared, people started to apply GaN material in electrical devices. In 1991, the first blue LED appeared [7], after that, InGaN-based high brightness blue LEDs [8][9], and InGaN-based laser diodes appear in turn[10]. It turns out the GaN-based LED has a longer lifetime, and higher efficiency than traditional incandescent lights and fluorescent lights that were most widely used. The application of Ga-based LEDs would save a lot of energy for the world as the lighting cost takes a big portion of human energy consumption. For that reason, GaN became a highly valuable material that catches a lot of attention in the research of its properties.

1.1.2 Future of GaN material

Despite the prosperity of the GaN material market, there is still more potential to reveal in this material. There's an interest to grow InN/GaN heterostructures as the big difference between the band gap of GaN and InN would create a strong confinement of electrons[11], on the other hand, the small band gap of InN would broaden the material

emission range from ultraviolet to infrared. The whole visible range would be covered. However, the development of GaN/InN heterostructure is limited by the lack of a low-temperature GaN growth technique. The currently used GaN grow temperature is 800C, under which temperature InN would decompose. Therefore, the development of InN/GaN heterostructure depends on the development of a low-temperature GaN growth technique. The mobility of Ga atoms on a growing surface would be low at low temperatures, therefore the possibility of forming Ga vacancy increases that make the reason against low-temperature growth. In order to solve this problem, a new method of low-temperature GaN growth technique was proposed. This technique is called metal modulated epitaxial (MME) growth [12]. In this method, Ga and N are supplied to the growth surface at the same time using a Ga flux much greater than is required for stoichiometric growth. After a few nanometers of GaN growth, Ga metal accumulates on the surface. In order to incorporate this excess Ga, the Ga flux is shuttered off and the N flux crystallizes it into several more monolayers of GaN. Then the process is repeated until the full growth thickness is achieved. Under these conditions, the GaN growth was in Ga-rich and N-rich alternatively, it is expected Ga vacancy would be less likely to happen under this condition. However, the optical characteristic of materials grown by this method is not fully understood yet.

1.2 Methodology

In order to detect the property of GaN material without destroying its structure, the most popular way is to take a photoluminescence (PL) measurement on the material. When a laser beam was illuminated on the material, the electron would be excited to a high energy state, this energy state is unstable, so it will decay to a low energy state after a

very short amount of time and given out a photon. This process is called photoluminescence. Observing the PL spectrum will give us a lot of information about the electron energy state in the solid.

1.2.1 Optical properties of GaN

GaN material can have either zincblende or wurtzite structure with band gaps of 3.27eV and 3.478eV respectively. As wurtzite GaN is more stable, it attracts more attention from scientists. The structure of wurtzite GaN is shown in Figure 1-1:

1.2.2 Growth of GaN

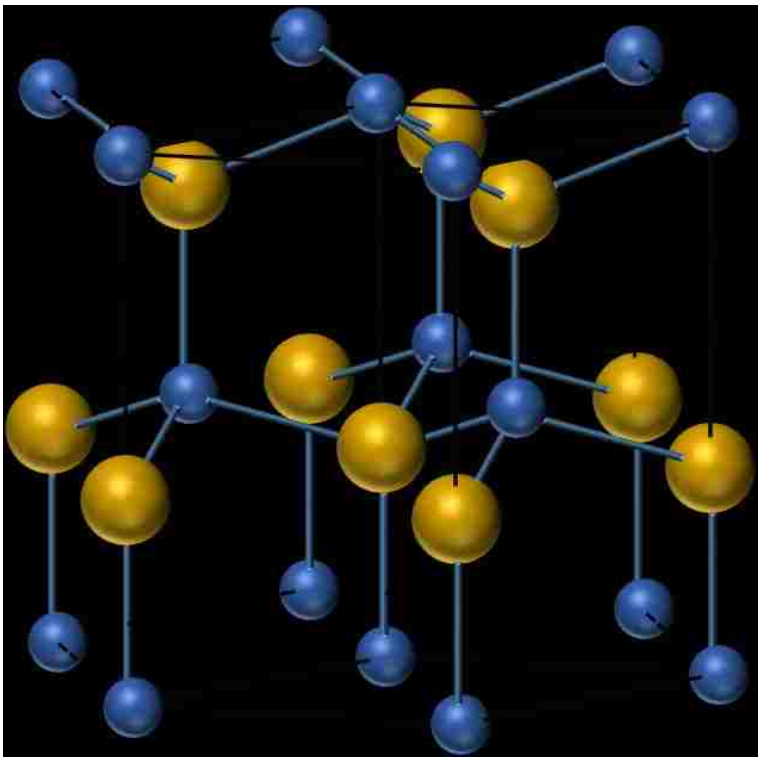

The melting point of GaN is 2300℃, so the growth of GaN has to happen at very high temperature, which makes the growth of GaN relatively expensive. The growth technique

of GaN has developed a lot from 1969 to date. There are three types of growth technique widely used in current time. They were MOCVD method, MBE method, and Hydride vapour phase epitaxy (HVPE) method. Among those methods, MBE has the slowest growth rate and the highest cost, but at the same time also has the most precise control on deposition thickness and surface structure. So this technique is widely used for research. The other two type of method has their value for business use.

The MBE growth of GaN uses Ga metal as the Ga source and N ion from a plasma as the N source. The molecular beams of Ga and N react on the substrate surface and form GaN epitaxial film. The whole process has to happen in a high vacuum chamber in order to get pure material. During the growth process, the Ga/N ratio, substrate temperature, and growth rate have a great influence on GaN morphology.

1.2.3PL measurement of GaN

The current GaN growth technique is not perfect, the quality of the GaN crystal is greatly affected by the large dislocation density and intrinsic defect density. The crystal quality of MBE grown GaN is much lower than GaAs crystal. The existence of crystal defects destroys the periodic structure in GaN lattice and affects the energy structure of electrons. The electrons trapped by defect centers usually have lower energy than electrons in the conduction band, therefore the defect has an added new energy band in the GaN band gap. Those new energy levels may be radiative or nonradiative recombination centers, changing the fluorescence of the GaN material. On the other hand, analyzing the property of defect emission helps us to tell the quality of GaN material by looking at its spectrum. A lot of research has been done to examine the property of GaN by looking at its PL. It

provides us a base of information to build a connection between PL characteristic and GaN property like defect type, and defect density.

1.3 Content in this work

This work is inspired by the interest of understanding the optical properties of MME grown GaN by PL measurement method. In this thesis, the theory about fluorescence of GaN semiconductor would be described in Chapter 2, which contains the recombination theory and thermal equilibrium theory. They will be used to predict the relationship between GaN material and its fluorescence spectrum. In chapter 3, the techniques and experiments used in this research are described. In chapter 4, the PL measurement on GaN template, GaN buffer layer, and MME grown GaN cap layer will be presented. By comparing the PL of those samples, the signal from MME grown GaN cap would be identified. In chapter 5, the temperature dependent and power dependent PL measurements of the MME grown GaN cap layer will be analyzed, which provides more clue to identify the origin of each signal in PL, and therefore makes it possible for us to provide a prediction of GaN growth quality. At the end, we have grown a series of samples which has In droplet deposition between the GaN buffer layer and the MME grown GaN cap. The PL of those samples are presented in Chapter 6. Looking at the PL of those samples we have found that the In droplet deposition has reduced the formation of one type of defect which appears in MME grown GaN, however, the general quality of the cap layer still needs to be improved if it is expected to be used in a heterostructure. Finally, we conclude with the possible reasons that caused the quality degradation in cap layer and provided the suggestions on further research.

Chapter 2 Theory

2.1 Introduction

In this chapter, I am going to introduce the most relevant theories to explain the optical properties of GaN. I will start by introducing the concept of photoluminescence. Then I will explain the defect states in GaN, and how to explore defect properties of defects through excitation power dependence PL measurement and temperature dependence PL measurement.

2.2 Photoluminescence

When a semiconductor bulk is illuminated by short wavelength light (the energy of the photon has to be larger than the bandgap of the semiconductor), electrons will be excited to the conduction band and leave holes in the valence band. The resulting high energy electrons are unstable and will subsequently decay back to their low energy state. This decay is called the recombination of electron-hole pairs because in this process an electron finds a hole and both effectively disappear at the same time. The recombination process has to give out energy in order to conserve the energy of the whole system. Different ways of giving out energy differentiate the recombination process into three types. The first one is radiative recombination which gives off energy through the emission of a photon. The kinetic energy of the electron transfers to the photon energy. The second one is non-radiative recombination, which gives off energy by causing the lattice to vibrate. We also describe this process as creating phonons, because the quanta of vibration of a lattice is a phonon. In this case, the energy of the electron transfers to thermal energy. The third process is a so-called Auger process through which the extra

energy of the excited electron is given to another electron. As a result, the other electron is excited to a higher state. In this case, however, the excited electron doesn't usually take all the energy of the decaying electron, and it also must relax through some thermal transfer to lattice vibrations. In all, though these three processes are not independent and two processes can affect one electron. For example, a recombination process can create (or absorb) a phonon first then give off a photon. In principle, though by studying the emission of these photons, we can learn something about the electron states in the structure.

2.3 Thermal equilibrium

GaN is normally found to have a very high background electron concentration of 10^{18}cm^{-3} [13]. This large excess of electrons occupies the multiple energy states in GaN following the thermal statistics. Following laser light illumination of GaN, electrons are excited into higher energy states, and the original thermal equilibrium is broken. The relaxation and thermal equilibrium that follows is described in the following process.

Looking at n-type GaN containing a radiative acceptor level A_i with concentration N_d, laser light illumination of sufficient energy injects photogenerated carriers into the conduction band. Following this, they can become captured by the acceptor level, or form an exciton. The distributions of carrier concentrations in each level are determined by the following processes:

1) For the conduction band, electrons are generated optically at the rate $G(\text{cm}^{-3}\text{s}^{-1})$, adding δn to the "dark" electron concentration, making the total electron concentration $n = \delta n + n_0$.

2) For the acceptor level, electrons will be captured at the rate $C_{na}N_a n$, where C_{na} is the electron capture coefficient for the acceptor, N_a is the density of acceptor level, and n is the concentration of electrons in the conduction band. When the acceptor level captured an electron it will form a bound exciton, which recombines at the rate of $\frac{N_a^0}{\tau_{R_a}}$, where N_a^0 is the density of excitons bound to acceptor level, τ_{R_a} is the radiative lifetime of that state. The holes leave the acceptor level at the rate of $Q_a N_a^0$ due to thermal activation, where Q_a is the probability of exciton dissociation, which is proportional to $\exp(-E_A/kT)$, where E_A is the thermal activation energy for the radiative acceptors.

3) For the exciton level, excitons are formed with the rate $C_{ex}np$, where C_{ex} is the efficiency of exciton formation. The exciton would disappear through recombination at the rate of $\frac{N_{ex}}{\tau_{R_{ex}}}$, where N_{ex} is the density of excitons and $\tau_{R_{ex}}$ is the exciton radiative

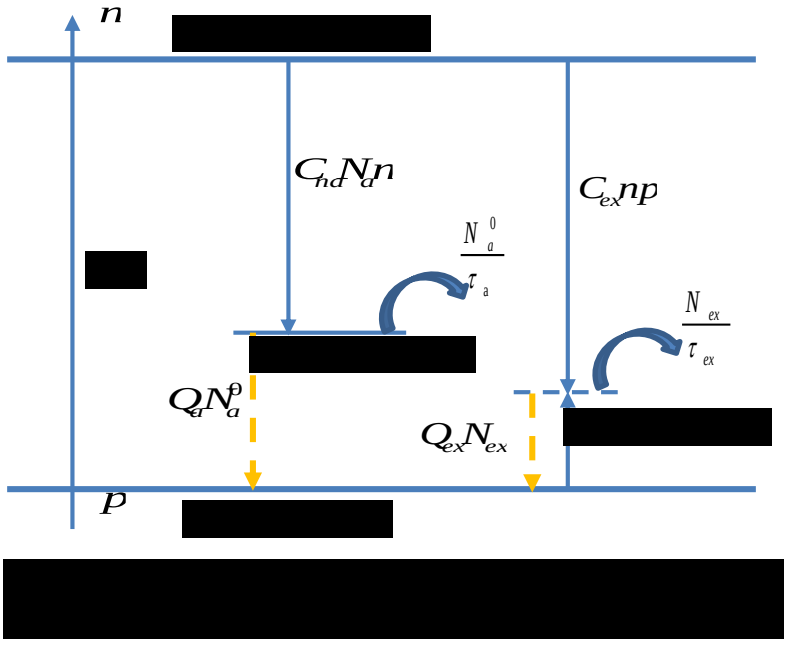

lifetime. The exciton can also dissociate, non-radiatively, with probability Q_{ex}, at a rate of $Q_{ex}N_{ex}$ due to thermal activation.

A schematic of the process described above is shown in Figure 2-1. At steady state we set the time variation equal to zero and can write the following balance equations for each level:

$$\frac{\partial p}{\partial t} = G - C_{na}N_a n + Q_a N_a^0 - C_{ex} np + Q_{ex}N_{ex} = 0 \tag{2-1}$$

$$\frac{\partial N_a^0}{\partial t} = C_{na}N_a n - \frac{N_a^0}{\tau_{R_a}} - Q_a N_a^0 = 0 \tag{2-2}$$

$$\frac{\partial N_{ex}}{\partial t} = C_{ex} np - \frac{N_{ex}}{\tau_{R_{ex}}} - Q_{ex}N_{ex} = 0 \tag{2-3}$$

With the above equations, the expression of the intensity of PL via the defect and the exciton can be written as:

$$I_d^{PL} = \frac{N_a^0}{\tau_{R_a}} = \frac{C_{na}N_a n}{1+\tau_{R_a}Q_a} \tag{2-4}$$

$$I_{ex}^{PL} = \frac{N_{ex}}{\tau_{R_{ex}}} = \frac{C_{ex} np}{1+\tau_{R_{ex}}Q_{ex}} \tag{2-5}$$

The probability of thermal activation Q_i is proportional to $\exp(-\frac{E_i}{kT})$, where E_i is the thermal activation energy of that level.

At low temperatures, the thermal activation of these levels is very small so that we can ignore this process. However, when the temperature is increased such that kT is comparable with the activation energy, most carriers will be thermally activated, and therefore the PL intensity will be greatly reduced. We can see this process in the following graph:

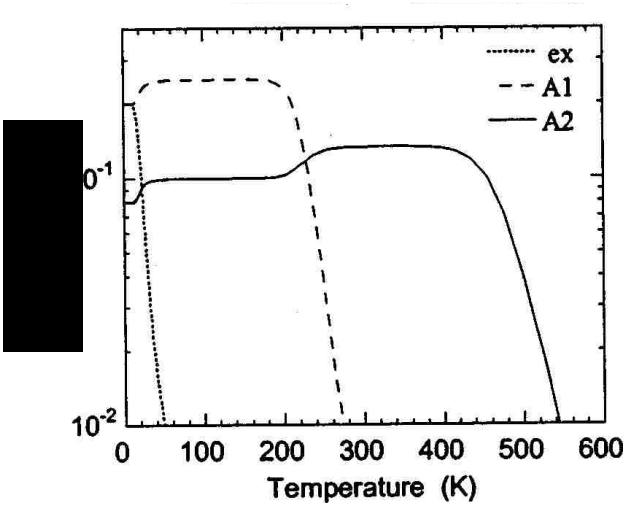

Figure 2-2 Calculated temperature dependencies of the PL intensity for three radiative recombination channels in GaN: excitonic and via two acceptors (A1 and A2). Adapted from ref 14.

The PL intensity of both the exciton and defect states decrease dramatically when the temperature reaches the appropriate critical value. By fitting the PL intensities of the respective emissions to the above equations we will extract the thermal activation energies for the exciton and the acceptor levels.

2.4 Electron states in bulk GaN

The periodic nature of all crystals allows us to describe their electronic states, GaN, in this case, using band theory [错误!未定义书签。]. The more stable form of GaN has the wurtzite structure with a direct the bandgap of GaN is 3.48eV at 0K [错误!未定义书

签。]. With increasing temperature, the lattice constant will expand, consequently, the bandgap energy will change and is described by the Varshni's formula [14]:

$$E_g = E_0 - \alpha T^2 / (T + \theta_d) \quad (2\text{-}6)$$

Where α and θ_d are fitting parameters, E_0 is the bandgap at zero temperature, E_g is bandgap at temperature, T. Due to limitations in the current technology of bulk GaN crystal growth, our MBE grown crystal films have relatively high lattice defect densities which propagate from the substrates they are grown on. These defects include but are not limit to dislocations, stacking faults, and impurities. When a defect is formed in a crystal, the periodic structure of the lattice is affected. The area around the defect center will have a distorted energy field. Electrons around the defect center usually have lower energy than free electrons and can become trapped by the defect entering defect levels which can exist within the bandgap [15].

There are several specific intrinsic defects which are commonly found in GaN. They are:

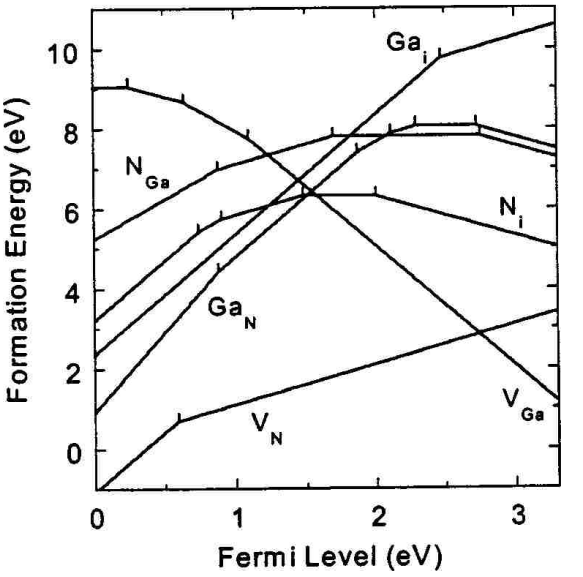

[redacted]

Gallium vacancy (V_{Ga}), Nitrogen vacancy (V_N), Gallium antisite (Ga_N), Nitrogen antisite (N_{Ga}), Gallium interstitial (Ga_i), and Nitrogen interstitial (N_i).

The formation energy of these defects have been calculated through first principle calculations by [13] and are shown in Figure 2-3 as a function of the chemical potential. For defects with multiple possible charge states, only the state with the lowest formation energy is shown in the graph. The slope of each line indicates the amount of charge. The X axis represents the Fermi energy above valence band maximum. As it shows in the graph on the right-hand side, when GaN is grown under heavily n-type conditions, i.e., with the Fermi level near the conduction band, the V_{Ga}^{3-} has the lowest formation energy. This is the case for initiating growth on commonly used Undoped GaN template substrates. The transition energy of each defect is shown in figure 2-2. From here we can see that V_{Ga}^{3-} has an energy level of 1.1eV. Therefore, a radiative transition between the

conduction band and the V_{Ga}^{3-} defect state will give off emission at 2.2eV, corresponding to a yellow light emission. This contributes to the well-known "yellow luminescence" band in GaN [16].

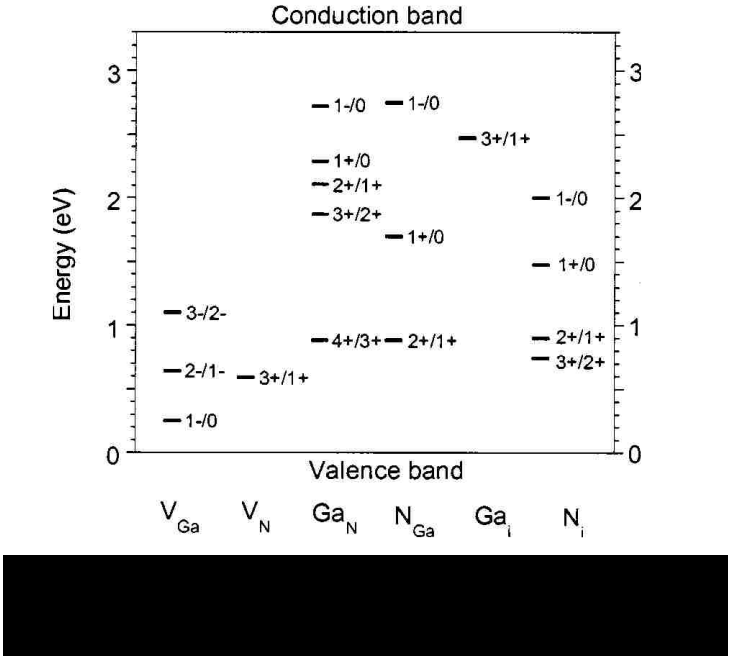

2.5 Free carrier generation and recombination process

Because of the existence of lattice defects, the electrons in GaN not only occupy the energy states near the band edge, but they also occupy the defect states, localized around the defect centers. When an electron decays from one energy state to another, a photon can be emitted to compensate the energy difference between the states. This process can be described as the recombination of an electron from a higher energy state with a hole from a lower energy state. Including defect states, several possible recombination channels in GaN are described by the following figure.

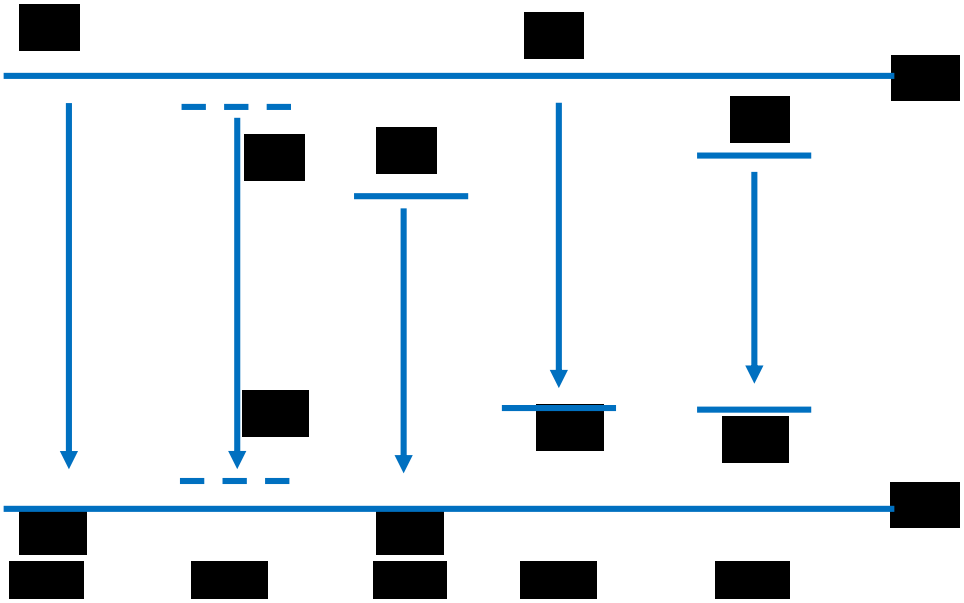

Figure 2-5 Energy level diagram of GaN, possible recombination channels are indicated with an arrow. Each letter at the bottom of the figure stands for one type of recombination channel.

Recombination processes [17]:

a) Band to band transition <eh>, free carriers from the conduction band and valence band recombine with each other, producing photons with energy:

$$\hbar\nu = E_g \tag{2-7}$$

b) Free exciton transition <FE>, an electron and a hole become bound to each other forming a stable exciton. This recombines producing photons with energy:

$$\hbar\nu = E_g - \frac{m_r e^4}{2h^2\epsilon^2} \tag{2-8}$$

Where $\frac{m_r e^4}{2h^2\epsilon^2}$ is an estimation of the binding energy of exciton.

c) Recombination between a hole and an electron bound to a neutral donor<D0 h> produces a photon energy of:

$$\hbar\nu = E_g - E_d \tag{2-9}$$

Where $\boldsymbol{E_d}$ stands for the binding energy to a donor center.

d) recombination between an electron and a hole bound to a neutral acceptor<A0 e>, produces a photon energy of:

$$\hbar\boldsymbol{\nu} = \boldsymbol{E_g} - \boldsymbol{E_a} \tag{2-10}$$

Where $\boldsymbol{E_d}$ stands for the binding energy to an acceptor center.

e) Donor acceptor pair transition<DAP>, an electron bound by a neutral donor level recombines with a nearby hole bound by a neutral acceptor level:

$$\hbar\boldsymbol{\nu} = \boldsymbol{E_g} - \boldsymbol{E_a} - \boldsymbol{E_d} - \frac{\boldsymbol{e^2}}{\boldsymbol{\epsilon r}} \tag{2-11}$$

Where $\frac{\mathbf{e^2}}{\boldsymbol{\epsilon \mathbf{r}}}$ stands for electrostatic potential between electrons bound to donor center and holes bound to acceptor center. $\mathbf{r}$ Stands for the distance between donor center and acceptor center.

Some of the defect centers are nonradiative [18]. Alternatively, phonons would be given out to compensate for the energy loss in the recombination process.

2.6 Effect of excitation power

As shown above, the dependence on the excitation power through G in Eq. 2-1, can, in general, be complex. It has been reported that the emission intensity of the free exciton or bound exciton in GaN will vary as a function of the excitation power with between a 1st and 2nd order power law [19], while the power dependence of donor-acceptor pair recombination or recombination between a free carrier and a defect level would have a power law between 0.5~1st order [19]. T. Schmidt calculated the power dependence of the

PL by taking account of the transitions shown in Figure 2-5[19]. Following is a description of his methods. Assuming a relatively high-intensity laser excitation ($\sim 1.8 W / \mu m^2$), we can neglect the intrinsic carrier concentration and let the electron concentration, n, in the conduction band be equal to hole concentration, p, in the valence band. Here we strictly define n and p as free electrons and free holes respectively. Once the electron and hole forms an exciton it no longer count into n and p. With above definition we then make the following assumptions:

1) For recombination through exciton transitions, there are three transitions: free-exciton recombination, and donor or acceptor bound exciton recombination. For this type of transition, the intensity of PL can be written as:

$$I = \frac{n_e}{\tau_e} \propto n^2 \tag{2-12}$$

n_e is the amount of exciton. τ_e is the lifetime of the exciton. Since the possibility to form an exciton is proportional to $n \times p \approx n^2$, we can write the intensity of the exciton PL as proportional to n^2.

2) For recombination between a defect level and the band edge, there are two paths considered: recombination of a hole and an electron bound to donor center, or recombination between an electron and a hole bound to acceptor center. For this type of transition, the intensity of PL can be written as:

$$I = \frac{N_{D^0} * p}{\tau_d} \tag{2-13}$$

At steady state, there should be the same amount of electrons captured by defects as lost through recombination. So this equation could be written as:

$$g * n * N_{D^+} = f * N_{D^0} * p \tag{2-14}$$

The intensity of PL can be written as:

$$I = \frac{N_{D^0} * p}{\tau_d} = \frac{g * n}{g * n + f * p} * \frac{N_D * p}{\tau_d} \propto n \quad (2\text{-}15)$$

(g and f are capture coefficient of the defect levels for electrons and holes respectively)

3) For donor-acceptor pair recombination the process involves the capture of a hole by the donor level, the capture of an electron by the acceptor level, and finally, the recombination of the donor bound hole with the acceptor-bound electron. These processes are governed by the following equations;

$$I = \frac{N_{D^0} * N_{A^0}}{\tau_d} \quad (2\text{-}16)$$

$$\frac{N_{D^0} * N_{A^0}}{\tau_d} = g * n * N_{D^+} \quad (2\text{-}17)$$

$$\frac{N_{D^0} * N_{A^0}}{\tau_d} = a * p * N_{A^-} \quad (2\text{-}18)$$

(a, g and f are capture coefficient of the respective defect levels)

It's hard to get the exact power dependence index of donor-acceptor pair recombination through the above equation since the amount of available donor center and acceptor center actually depends on n. However, we can conclude the power dependence index should be smaller than the transition of defect level and band edge.

In the three types of process, I is either proportional to n or n^2. Which indicates the PL intensity would respond to excitation power with different power law due to different recombination channel. The relationship between n and excitation power G varies under different condition, it depends on which type of recombination is dominant, exciton recombination or free to bound recombination. In general, $n \propto G^{0.5\sim1}$. Hence the band edge emission usually have excitation power index of 1~2. A free to bound recombination

usually have power index of 0.5~1. Hence the power dependence measurement of PL can be used to identify recombination type.

2.7 Conclusion

In this chapter, we have discussed the carrier recombination processes in GaN. The light emission through different recombination processes shows different properties. In the form of different center wavelength, thermal activation energy and excitation power dependence. By making PL measurements of the thermal dependence and excitation power dependence we can identify the origin of light emission. Which provides a clue to understanding the material property, like the defect type and defect concentration in the material.

Chapter 3 Experimental techniques

3.1 Introduction

In this chapter, I will introduce the experimental techniques used in this research. Included is a brief description of molecule beam epitaxy (MBE), which is used to grow all of the samples studied here; atomic force microscopy (AFM), which is a high resolution technique to detect surface structure on the sub-nanometer scale; and photoluminescence (PL), which is used as an optical probe of the material system.

3.2 MBE technique

MBE is a technique invented by Cho et al in 1968 for thin film growth and is famous for producing high-quality crystal structures [20]. The key process of MBE is vacuum evaporation. Ultra-high purity atomic source material is heated in vacuum to generate an atomic flux. Then the flux travels through the vacuum to reach a substrate or seed crystal forming a thin film on it. Because the growth environment is in high vacuum, the mean free path of molecules or atoms is longer than the distance from the source to the substrate. As a result, we can control the growth of the crystal by controlling the flux density through the temperature of the source. This flux is governed by the following formula [21]:

$$J_i = [\frac{ap_i}{\pi d^2 (2\pi m_i kT)^{1/2}}]\cos\theta \qquad (3\text{-}1)$$

Where J_i is the flux per unit time at a distance, *d*, from the source, which has an orifice of area, *a*, and contains atoms of mass, m_i, have an equilibrium vapor pressure p_i at temperature T, k is the Boltzmann constant, and θ is the angle between the beam and

the normal axis of substrate surface. This flux is controllable down to a level where it allows for the growth of as small as one atomic layer at a time.

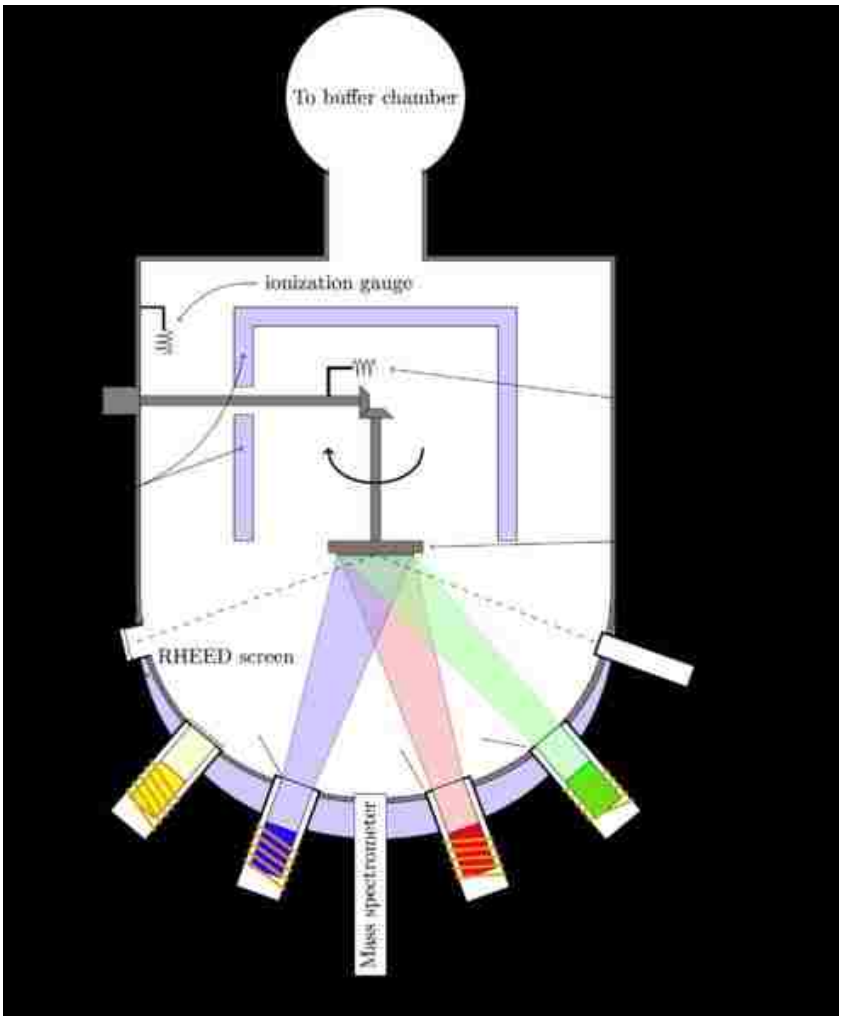

Figure 3-1 Schematic of MBE chamber [23]

The growth progresses through the following reactions: atoms are captured by the surface, and subsequently can either become mobile on the surface, desorb from the surface, or chemically bond to the surface becoming part of the lattice. The temperature of the substrate surface is a crucial element in this reaction. With high substrate temperature, the atoms have high enough energy to move to ideal incorporation sites.

However, if the temperature is too high the atoms may re-evaporate from the surface. With low substrate temperature, the atoms have low energy and low mobility. As a result, vacancy defects tend to form during growth.

Fig 3-1 [22] shows the following main components in MBE chamber:

- MBE sources: There are crucibles to store source materials, with a shutter at the end to control growth. It can be heated to generate the atom flux
- Substrate stage: The substrate stage is to hold the substrate. It is rotated to achieve more uniform growth.
- Electron gun and Rheed screen: The electron gun generates an electron beam which is incident on the substrate surface reflects off the substrate and hits the Rheed screen. The diffraction pattern from that reflection offers an image which gives a reciprocal space representation of the surface structure of the substrate.
- Beam monitoring Ion Gauge: The beam monitoring ion gauge measures the equivalent pressure of the source flux in the chamber.

3.3 AFM technique

Atomic force microscopy is a high-resolution imaging technique which uses the interaction between a tiny probe and the sample surface to map the topography of the surface. The following Figure 3-2 shows the components of an AFM machine.

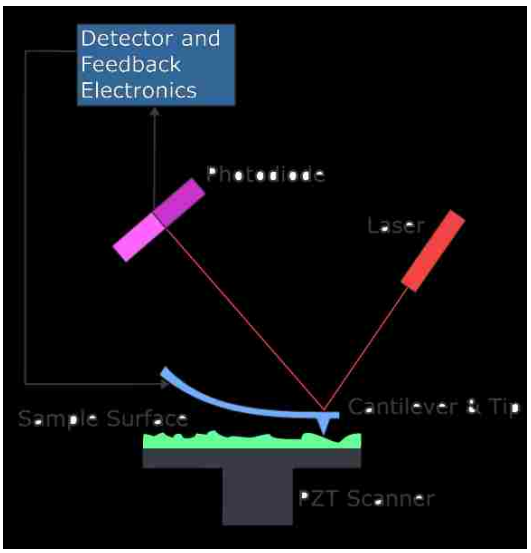

Figure 3-2 Key components of the AFM machine

The main components of an AFM is a cantilever with a tip, which has an end radius at the Nano-scale, a laser, a position detector and a moving stage. When the cantilever is moved close to the sample surface, the force between the cantilever tip and the atoms on the surface cause it to deflect which is detected by the laser. Moving the tip across the sample creates an image of the whole sample surface.

3.4 PL measurement

PL is a non-destructive technique which probes the electronic structure of semiconducting materials using light. The PL measurement system includes an excitation light source, a cryostat to keep the sample at low temperature, and a spectrometer to measure the spectrum.

3.4.1 Optical setup

The optical setup of the PL system is shown in Figure 3-3:

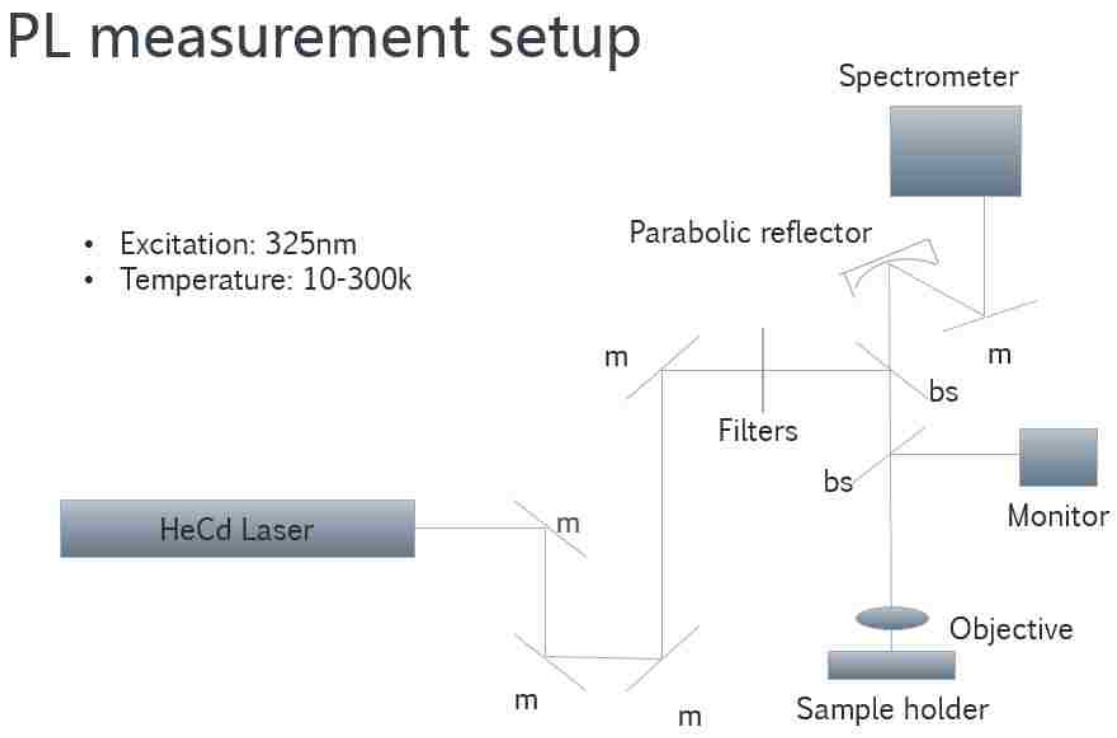

Figure 3-3 Optical setup of PL measurement

We used a HeCd laser whose center wavelength is 325nm to illuminate the sample. The laser beam is focused on the sample then collected by the parabolic reflector and focused onto the entrance slit of the spectrometer.

3.4.2 Spectrometer

The light detection system is a spectrometer with the optical path as shown in Figure 3-4. The input light beam enters the spectrometer through a slit with controllable size to shape the input light beam. Then the input light beam is reflected to a grating by a toroidal mirror. The grating can be changed to vary the dispersion in the spectrometer from a low dispersion 75 grooves/mm to a high dispersion 1200 grooves/mm. The slit size and

grating determines the resolution of the spectrometer. After the light is reflected by the grating, a large focusing mirror focuses the light on the exit port, where a CCD detector or IGA detector is placed to record the spectrum.

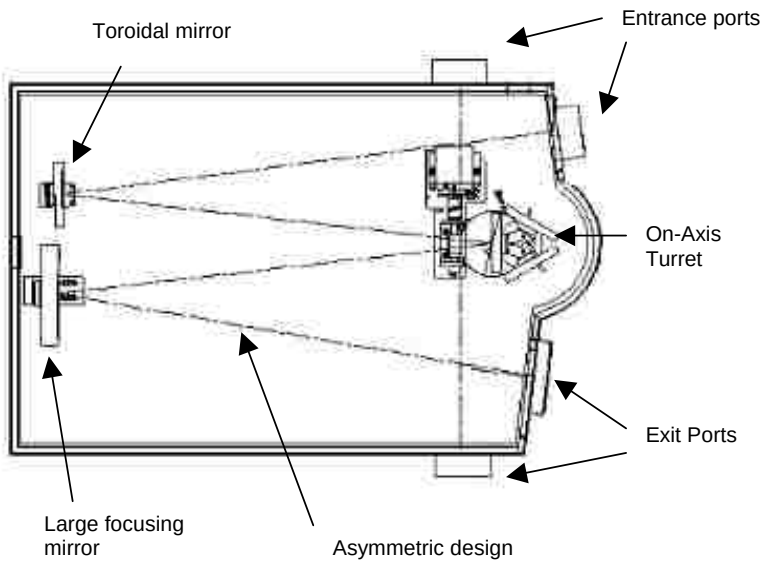

Figure 3-4 Schematic of spectrometer

3.4.3 Background light

When we measure the PL spectrum of the sample, there are several types of background light that we need to deal with. First, there can be light from the room entering the optical path of the measuring setup. This light should be unmistakable if we take a "dark" measurement with the excitation laser turned off. This light can be subsequently blocked from the system or identified and removed from the spectrum.

Second, the laser itself can create background light by interacting with the water molecules in air resulting in optical transitions of the air molecules. This is especially problematic for UV excitation. This type of background light won't be observed in the dark measurement. But, moving the laser line filter closer to the sample results in a

decrease of these background lines due to the shortened optical path between the filter and the spectrometer.

Chapter 4 Optical characterization of reference samples

MBE growth of GaN begins with a commercially available GaN template upon which is grown a thick GaN buffer. Finally, after any layers to be studied are grown, we grow a GaN cap layer on top of the film to be studied. Therefore, when we take PL measurements the PL signal contains information from all the layers. In order to understand the effects of the In deposition on the luminescent properties fo the MME cap in our samples, we have made measurements on the following series of reference samples: GaN template, GaN template with the buffer layer, and MME cap layer on top of the buffer layer. By comparing the signal from each sample we are able to recognize which part of the signal reflects changes in the quality of cap layer resulting from the inclusion of the In layer in the growth.

4.1 PL of the template sample

First, we measured the PL of the GaN template. This sample is a ~5μm thick HVPE grown unintentionally doped GaN film on sapphire. At a temperature of 10K, the GaN template was illuminated with 1.8W/cm^2 using a 325nm HeCd laser. The light-induced fluorescence of the sample is collected by the confocal optical setup introduced in chapter 3 and forms an image on the CCD shown in *Figure 4-1*.

From *Figure 4-1* we can see the PL spectrum of the GaN template has a very strong emission peak at ~3.47±0.014eV. On the longer wavelength side of the main peak, there are several smaller peaks, the intensity of those peaks are less than 1% of the strongest peak and the energy difference between neighboring peaks are 81±14meV . We conclude that the main emission peak is the GaN band-edge emission, since the energy of this peak

matches with the band gap of GaN at low temperature [23]. The small peaks to the right side of the main peak are assumed to be phonon replicas of the band edge emission [24]. Photons generated from band edge emission would scatter off the crystal lattice and re-emit another photon with less energy which forms the phonon replica peak. The energy difference between photon replica and the main peak should be the amount of energy it

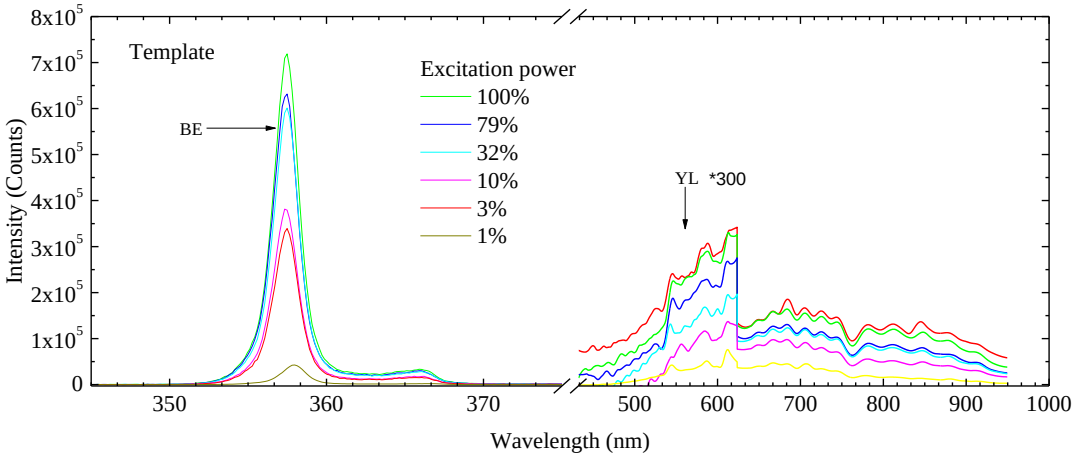

gives to crystal lattice in the form of a phonon. The value of the longitudinal phonon energy in GaN was reported to be 91meV at 0K [24], which is a close match to the 81 ±14 meV difference measured in this PL.

A significantly weaker emission band is found in the 450~800nm wavelength range for this GaN template. Which was reported as yellow luminescence by G. li *et al*. The cause of this emission is not clear since it appears in GaN materials grown by various techniques, it was accepted as an emission from Ga vacancy defects in GaN crystal. [16] The very low intensity of this band in comparison with the bandgap emission indicates a relatively low density of defects of this type [15].

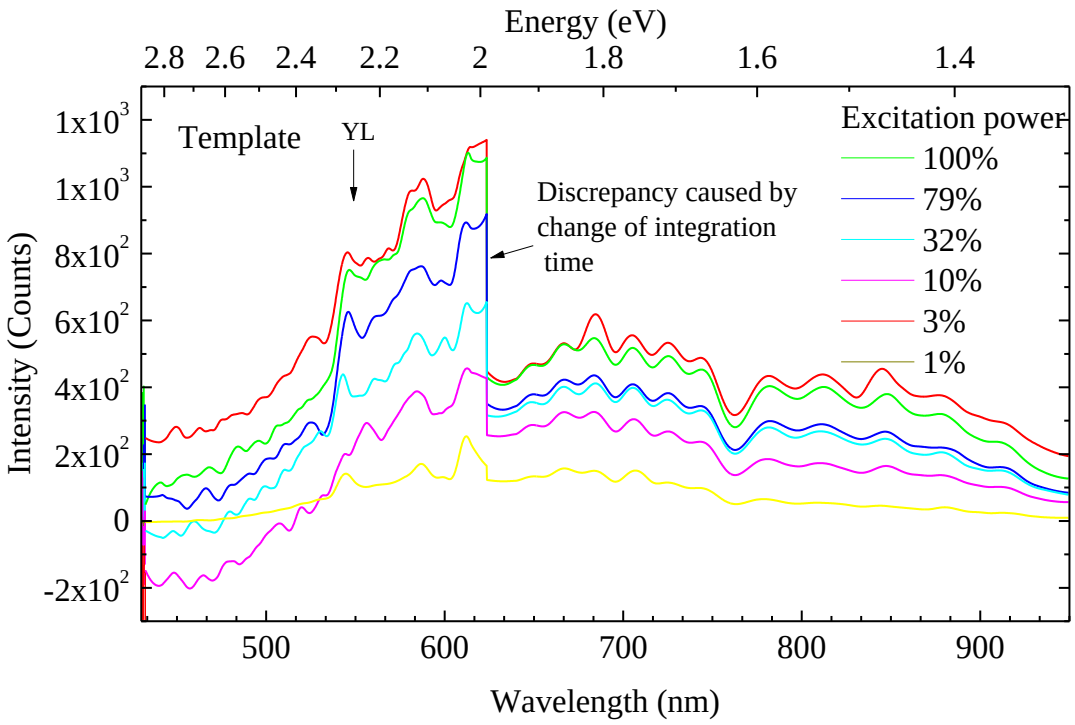

[redacted]

4.2 PL of GaN buffer layer

The reference sample with the traditionally grown MBE thick GaN buffer was also characterized with PL measurement. The GaN buffer was grown 100nm thick at a

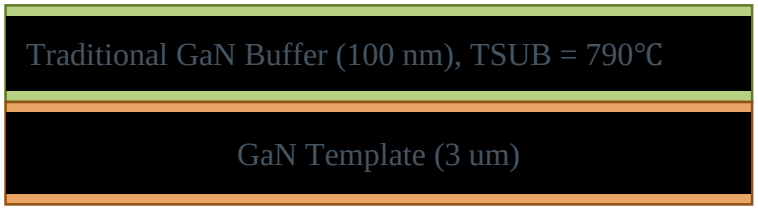

[redacted]

substrate temperature of ~790C. The structure of the reference sample is shown in *Figure 4-3*, the PL from this sample is shown in *Figure 4-4*.

In *Figure 4-4*, the band edge emission at 356nm still dominants the PL spectrum of GaN buffer layer. The phonon replicas were also observed at the same position. At the same time, there are two main emission bands at ~530nm and ~710nm which indicate the increased contribution of light from the defect centers from the buffer layer. The accepted absorption coefficient for GaN is 1.2×10^5 cm^{-1} at 325nm [25]. It follows that only 10% of laser light is absorbed by the buffer layer. The rest, ~90%, of the incident light is absorbed by the template. Therefore， the observed PL is a mixture of signals from both layers. In comparison with template GaN PL, the band edge emission from this sample has decreased by ~90%, while the defect emission increased about 1.9 times. This indicates that the buffer layer contains a significant density of defect centers that compete for emission with the band gap and can absorb the band edge emission from the template. The defect centers in the buffer layer can only partly explain the decline of band edge emission. If there is no other reason, the total amount of defect emission and band edge

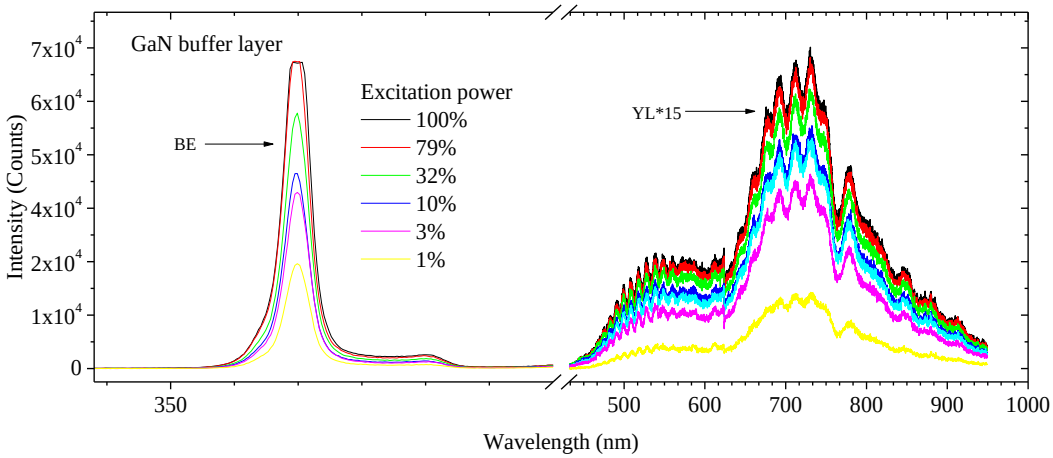

[redacted]

emission should be a constant for a constant excitation power, but that's not the case in our measurement, the total emission amount decreased by ~72%. Therefore we conclude that nonradiative defects exist in the buffer layer, which absorbs light from the band edge emission but does not re-emit it.

4.3 PL of MME grown GaN sample

Finally, we see the emission of the MME grown GaN reference sample. We performed PL measurements of sample NH55 which consisted of the following structure.

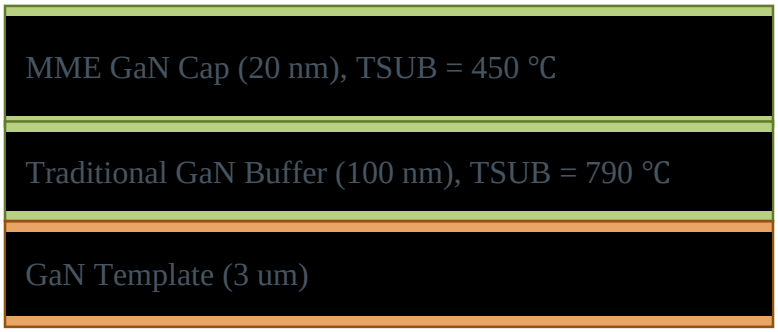

The sample started with an unintentionally doped template. Then, we grew 100nm GaN buffer layer at the traditional substrate temperature of 790 ℃. The sample was completed

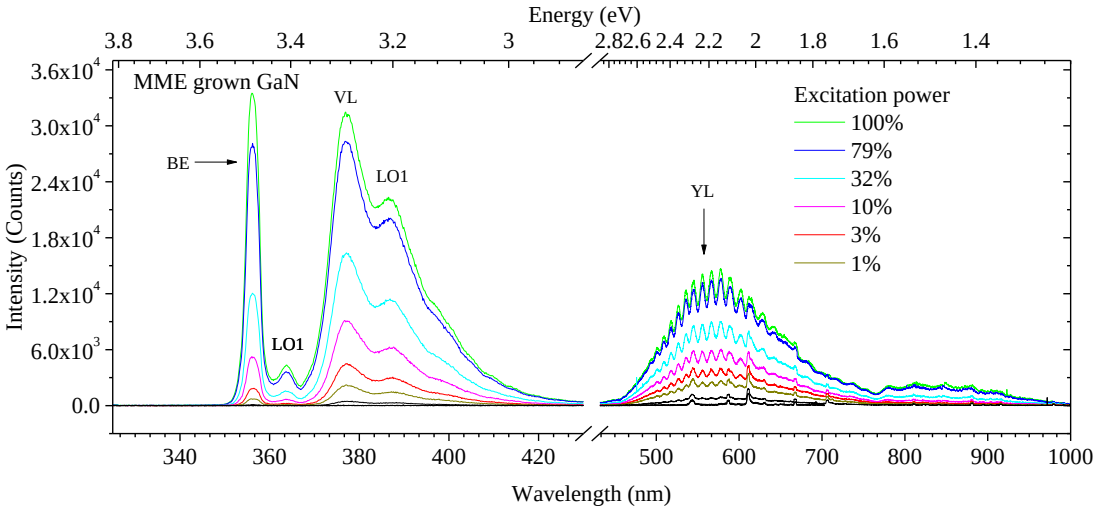

with a final cap deposition of 20nm of MME grown GaN at a substrate temperature of 450℃. PL of this sample is measured under the same conditions as above, except with a longer integration time of 10s. The result is shown in *Figure 4-6*.

In this PL, the band edge emission has greatly reduced in proportion to the 500~600nm defect emission band. The emission centered at 600nm became more dominant, suppressing the band edge emission. More importantly, a new emission peak at 340nm appeared. This indicates that the MME grown GaN layer not only creates more defects of the same type already seen in the traditional GaN, it also introduces some new type of defect. The details of this will be discussed in Chapter 5.

4.4 Summary

Comparing the PL of the GaN template, the high-temperature GaN buffer, and the MME grown cap layer, we can see that the GaN template has the highest quality in that the band edge emission is strongest there with little defect emission. For the GaN buffer layer, there is a slightly increased density of defects. However, for the MME GaN cap, a large increase in the defect concentration was observed, in addition to the introduction of a new type of defect level. If a low-temperature GaN Cap is to be used for InN/GaN hetero-structure, more research has to be done on the low-temperature cap to improve its GaN quality.

Chapter 5 Characterization of low-temperature MME cap emission

In the last chapter, we found a new type of defect signal in the luminescence of the MME grown cap layer. In this chapter, we will examine the temperature dependence and excitation power dependence of the PL from the reference sample with the MME grown GaN cap layer. Through these two types of measurements, we can get more information to diagnose the origin of all the defect state emission seen in the MME sample.

5.1 Analysis of the band edge emission

As a point of reference, we will analyze the band edge emission first. It is the result of the transition of free carriers from the conduction band to the valance band. From chapter 2 we know the energy of the band gap emission should be:

$$\hbar\omega = E_g - E_b \qquad (5\text{-}1)$$

Where E_b is the binding energy of the exciton, and E_g is the band gap of GaN. With this equation, the bandgap of GaN could be measured from PL. Since E_b was reported to be 21meV by Shan *et al*. [30].

5.1.1Temperature dependence measurement

Band edge emission from MME GaN cap layer was recorded at various temperature. The result is shown in Figure 5-1. It is observed from the PL that the band edge emission peak undergoes two types of change as the temperature increases. First, the intensity of PL decreases as temperature increase. Second, the energy of band gap emission decreases as temperature increase. According to the Varshni model [14], Eq. 2-4, the lattice constant of GaN increases as the temperature increases. This results in the narrowing of the band gap and the decrease in the band edge emission energy. The relationship between bandgap energy and temperature could be described by Eq. 2-6:

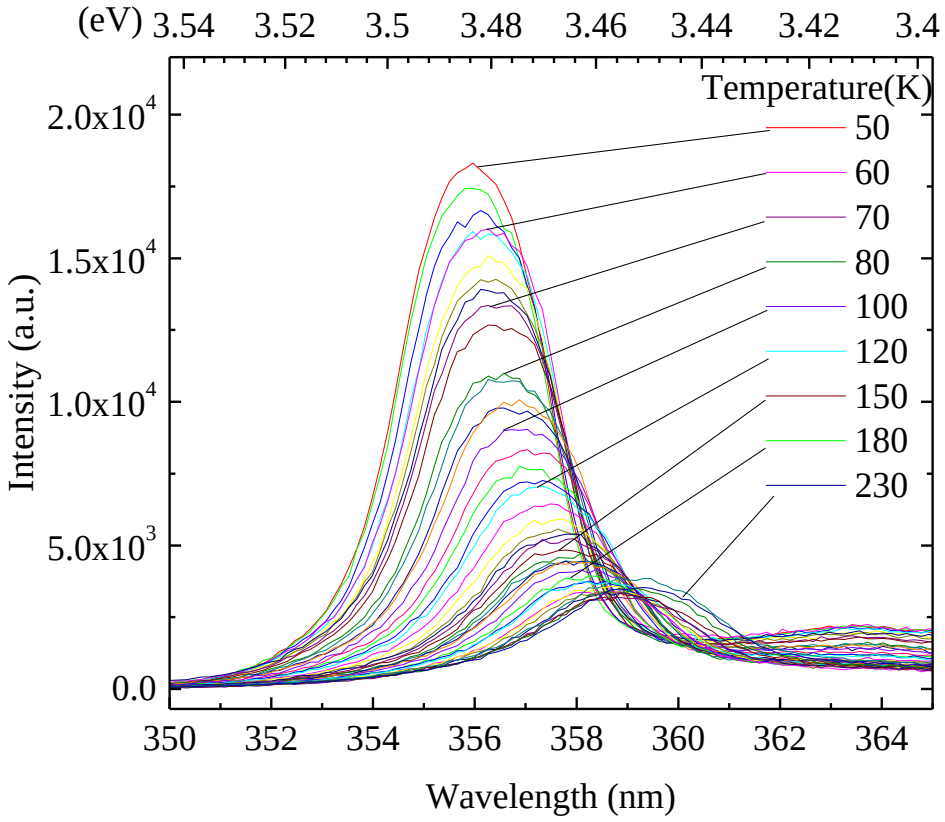

In order to correlate the data with Varshni's model, the band edge energy is calculated from equation 5-1 and plotted as a function of temperature in *Figure 5-2*. The experimental data was fitted to Varshni's formula, the result gives the fitting parameter $E_0 = 3.505\text{eV}$, $\alpha = 11.56\text{E-}4$, $\theta_D = 1187$. The bandgap value at zero temperature obtained from the fitting result matches well with reported value of GaN bandgap 3.478eV.[14]

From *Figure 5-2*, it is found that the experimental data diverges from the fitting curve when the temperature is above 130K. This divergence is caused by thermally activated exciton dissociation. The dominant recombination channel changes from exciton

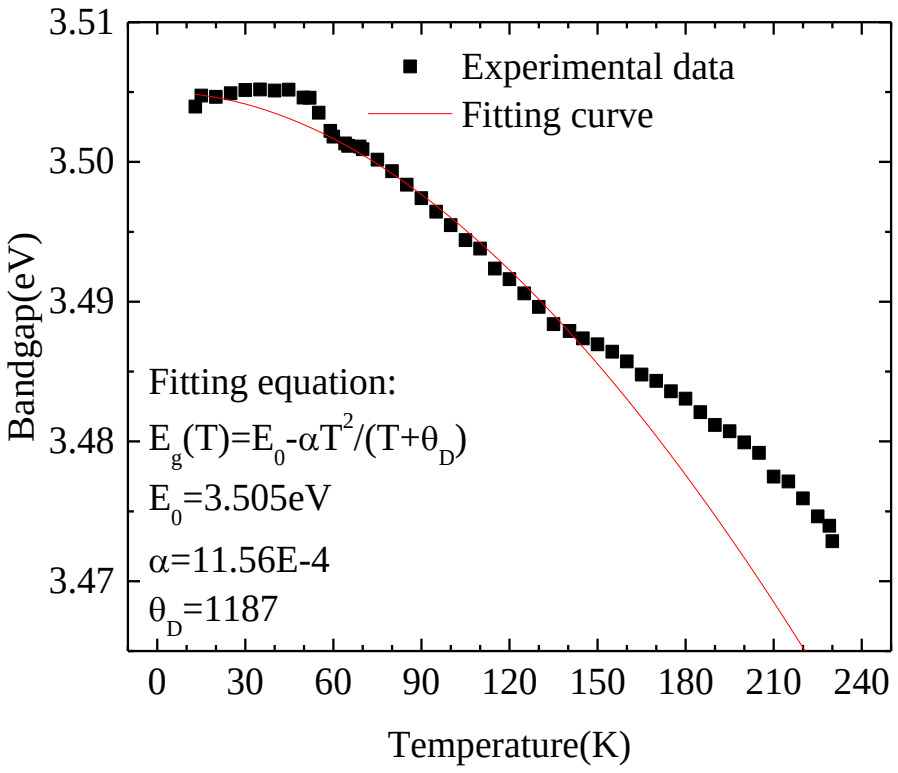

recombination to free electron and hole recombination when the sample was heated

above 130K. The thermal kinetic energy of GaN exciton is $2kT = 22.42\,\text{meV}$ (the number 2 stands for the two particles in an exciton, an electron and a hole), which is also a close match to the binding energy of GaN exciton. Which further supports this idea.

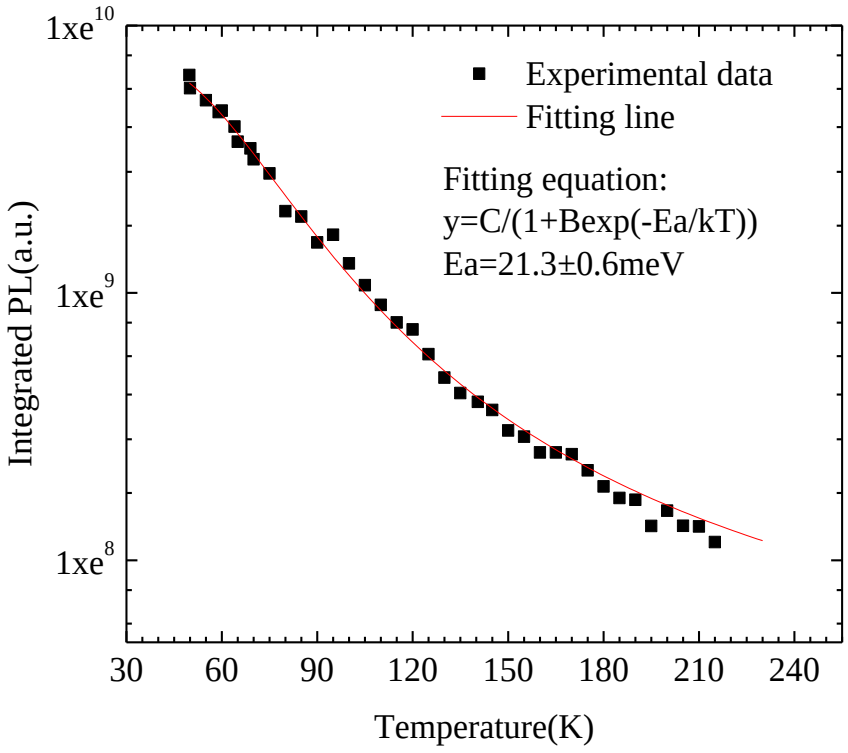

In 错误!未找到引用源。, the intensity of band edge luminescence was plotted as a function of temperature. Since the band edge recombination has lower efficiency than free exciton recombination, the intensity of PL would decrease as the dominant recombination channel changes from free exciton to band edge recombination. As it reflects on PL, the intensity of the PL peak will decrease as the temperature increases. This is the thermal quench behavior described in Chapter 2. The value of PL intensity could be described by the following equations:

$$I_{ex}^{PL} = \frac{N_{ex}}{\tau_{R_{ex}}} = \frac{C_{ex} np}{1 + \tau_{R_{ex}} Q_{ex}} \tag{5-2}$$

$$Q_e = C \exp(-\frac{E_{Ae}}{kT}) \tag{5-3}$$

Then the relationship between PL intensity and temperature can be simplified into the following equation:

$$I_{ex}^{PL} = \frac{C}{(1 + B \exp(-E_a / kT))} \tag{5-4}$$

Fitting the experimental data to this equation gives the fitting parameter of Ea=21meV, which matches well with the binding energy of the GaN exciton of 21meV, as reported by Shan *et al* [26].

5.1.2 Power dependence measurement

The band edge emission was also characterized as a function of excitation power, with the result plotted in *Figure 5-4*. This result shows that the PL intensity increases as the excitation power increases. The shoulder on the long wavelength side with less intensity is the phonon replica of the band edge emission. This originates from phonon scattering [24]. The energy of this peak is lower than the band edge emission because a phonon is scattered off when the photon is created.

The peak intensity of the band edge emission is plotted as a function of excitation power in *Figure 5-5*. The intensity of the excitation power is denoted as a percentage of the maximum power, which is 1.8W/cm^3 for our system. From the theory in Chapter 2, the

relationship between band edge emission intensity and excitation power should be described by equation 2-12.

$$I = \frac{n_e}{\tau_e} \propto n \times p \tag{5-5}$$

In general, photogenerated carrier density should be proportional to excitation power. Except GaN has n-type intrinsic defects, hence the density of electrons in GaN material won't change with excitation power. Then the relationship between PL intensity and excitation power should be:

$$L \propto I \tag{5-6}$$

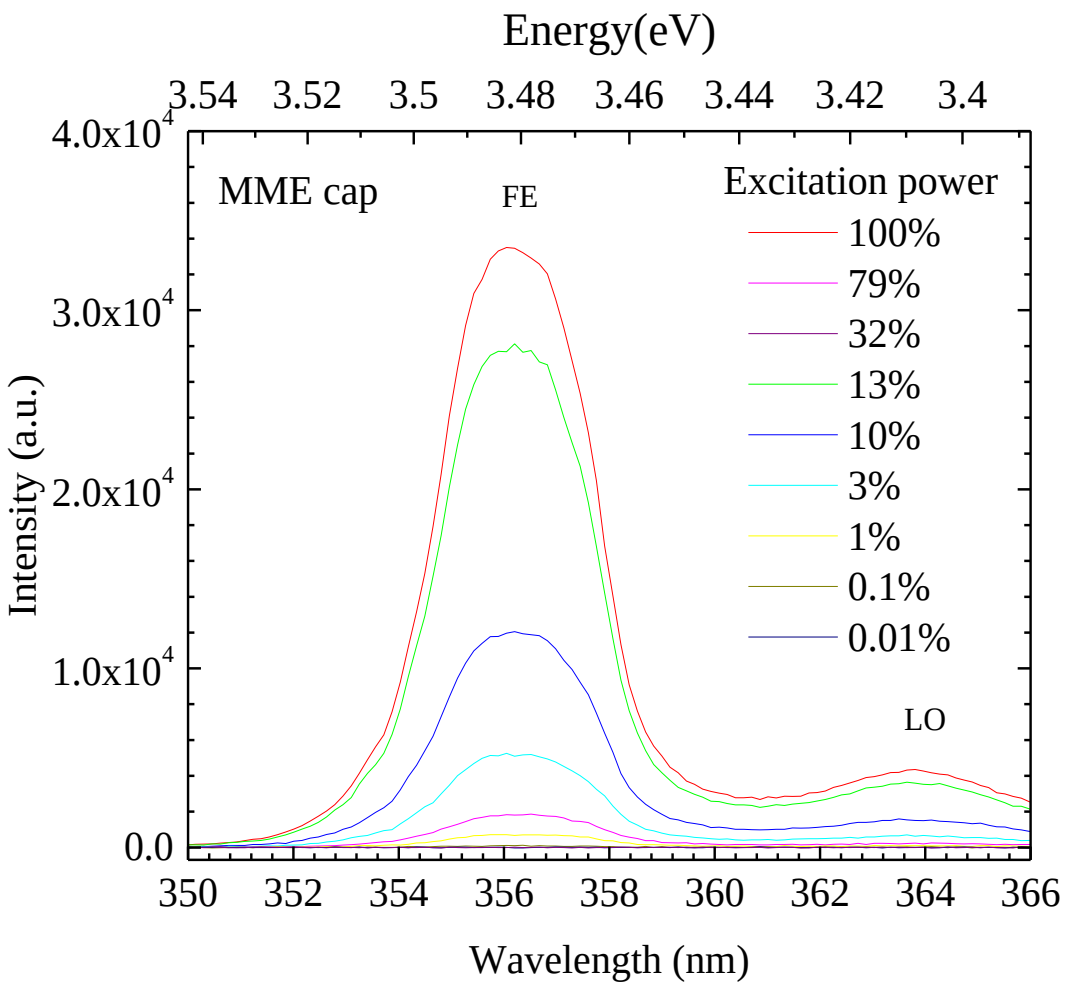

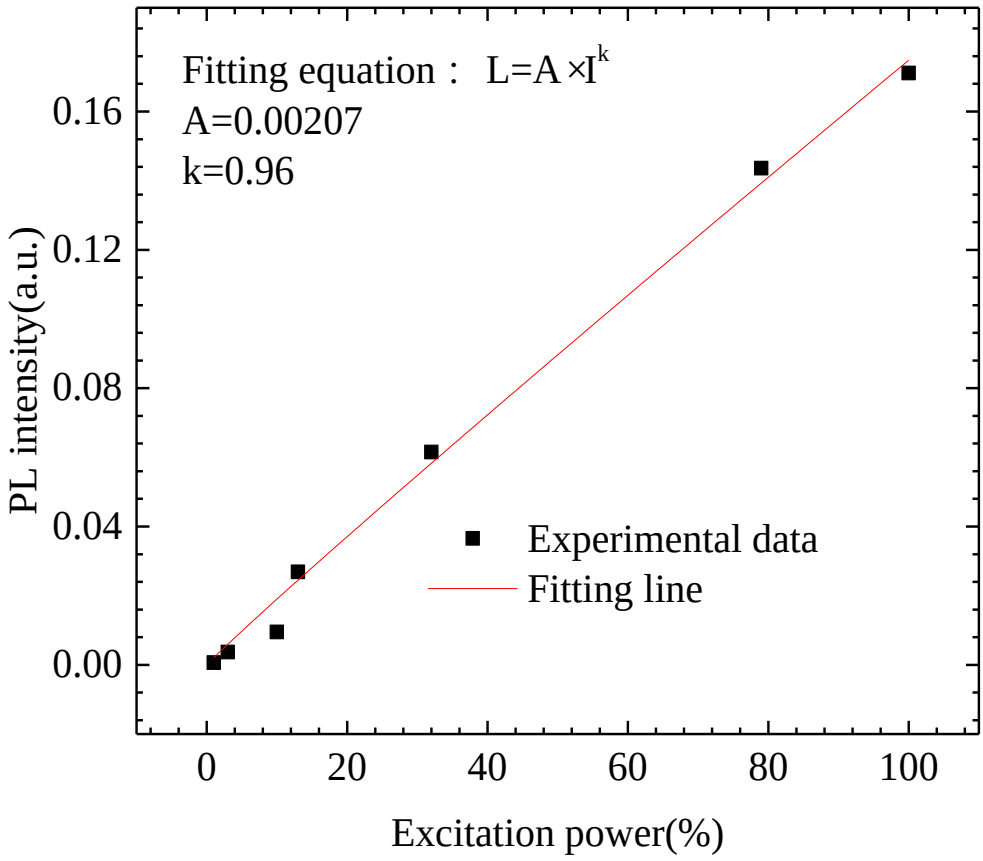

Fitting the power dependence data in *Figure 5-5* to the equation:

$$L = AI^{k} \qquad (5\text{-}7)$$

Where L means the intensity of PL, and I means the excitation power. The experimental data gives fitting parameter k=0.96.

5.2 Analysis of violet fluorescence

5.2.1 Power dependence measurement

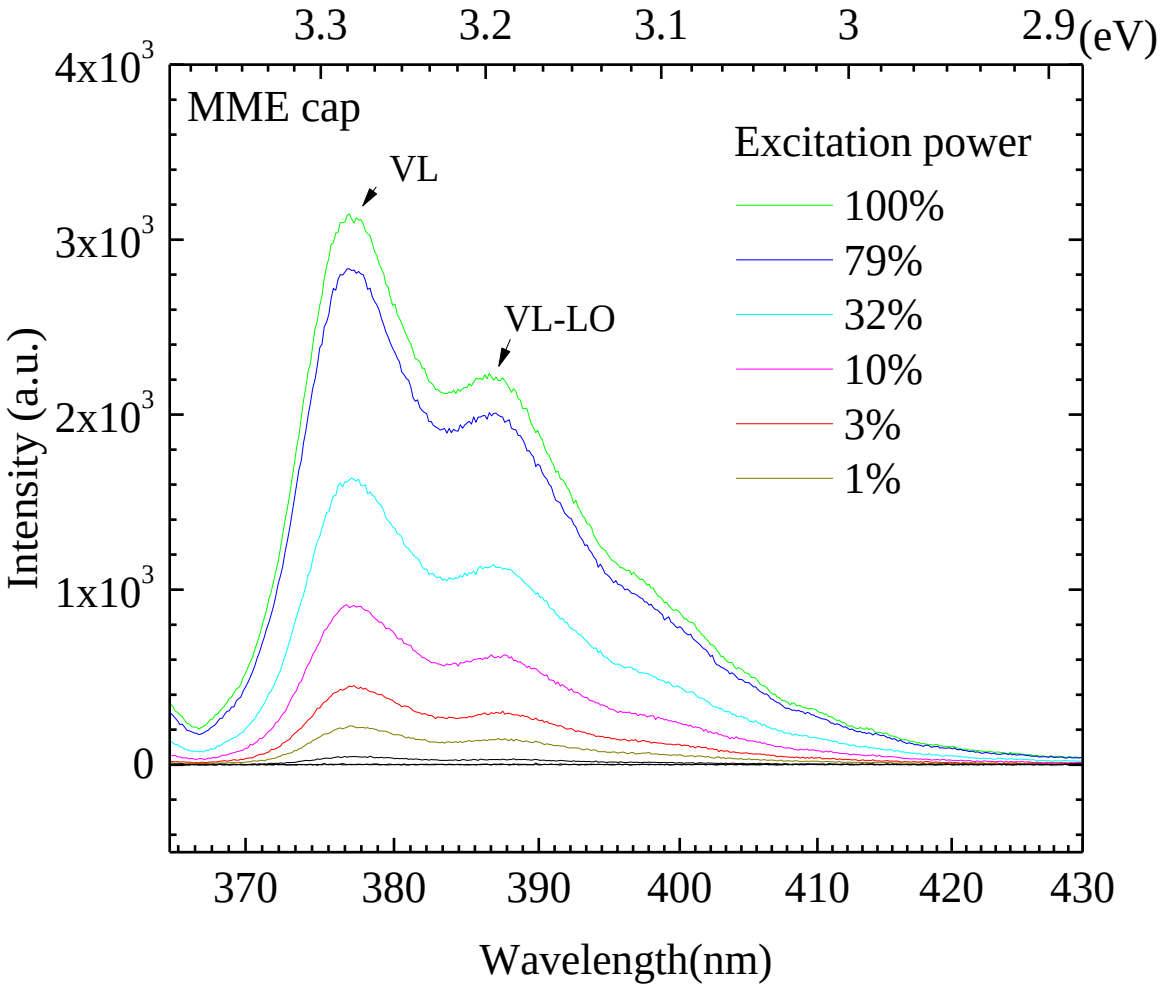

In the wavelength range of 365-430nm, the MME grew GaN has a PL emission band name violet luminescence (VL). The VL signal was characterized as a function of excitation power and is presented in *Figure 5-6*. The origin of this PL peak was assumed to be a new type of defect state that only appears in the MME grown GaN layer. Since the signal was not observed from the traditionally grown GaN buffer or the purchased GaN

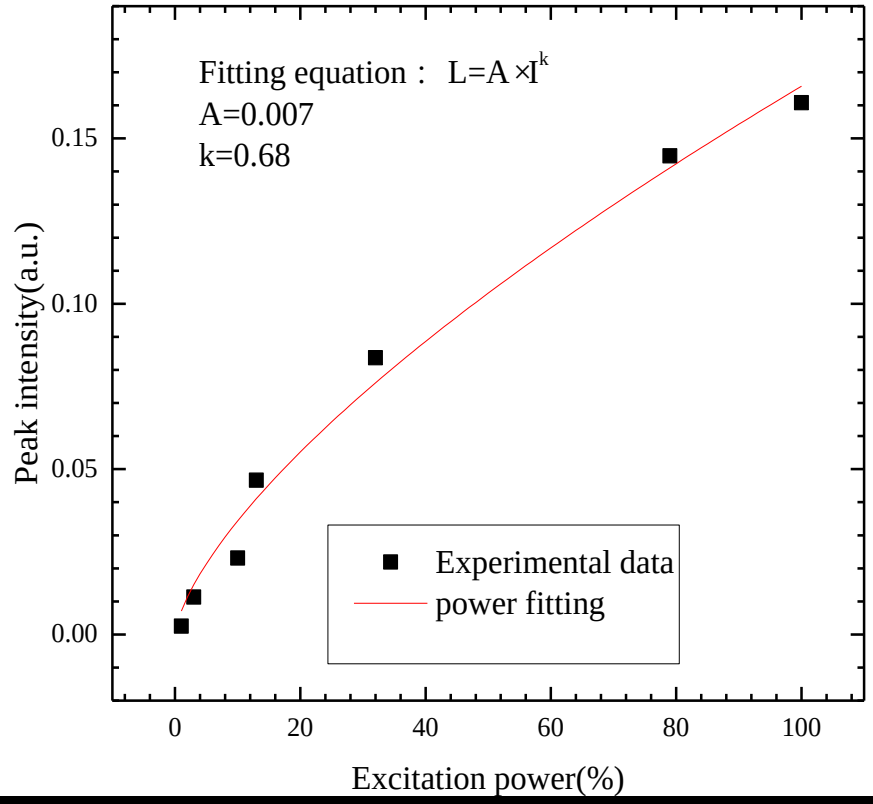

template. The two peaks in this wavelength range, and the extended low energy tail are believed to be due to phonon replicas, similar to the band edge peak. The first peak is centered at 3.29eV while the second peak is centered at 3.21eV. The difference between the two peaks is 80meV, which within the resolution (±13meV) of our system agrees with the phonon energy in GaN (91meV [23]). This can be continued throughout the low energy tail of the defect emission including several more phonon replicas.

The intensity of the VL peak is plotted as a function of excitation intensity in *Figure 5-7*, along with equation 5-8. The resulting fitting parameter, k=0.68, matches the prediction in Chapter 2.7 that the power index of defect emission should be less than that due to band edge emission.

5.2.2Temperature dependence measurement

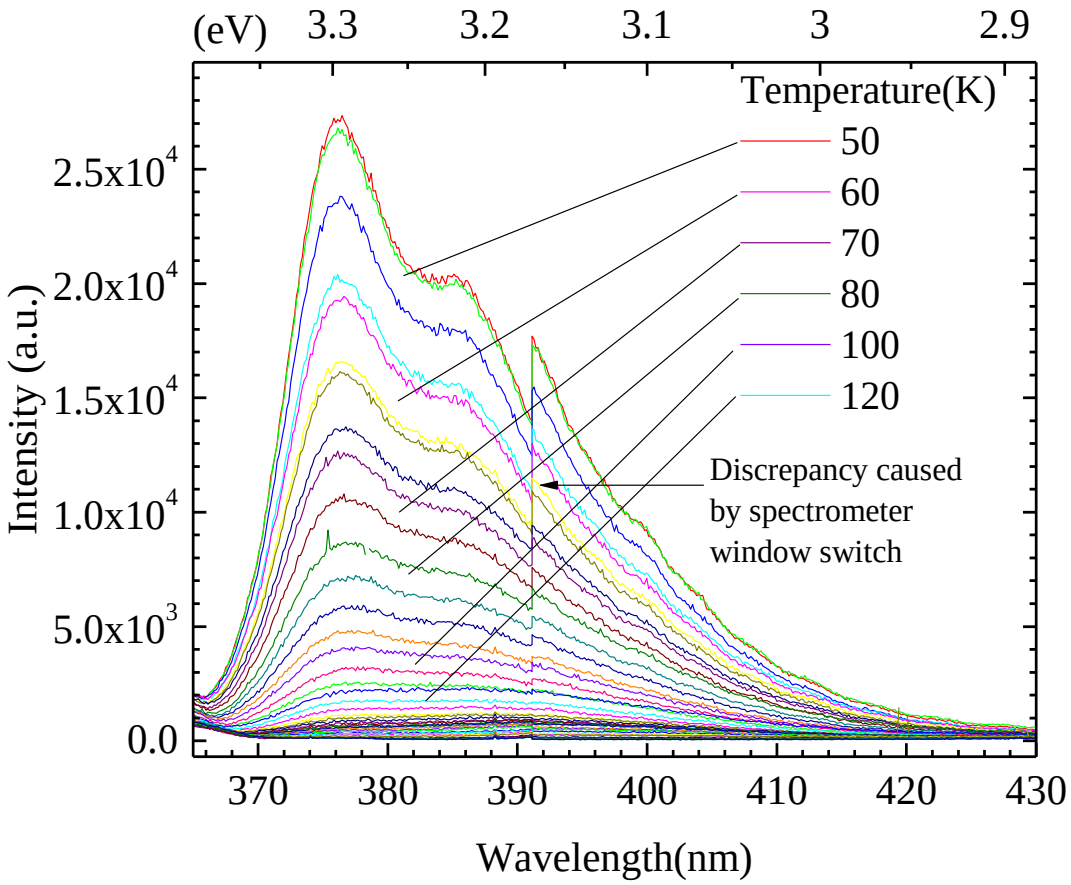

The VL peak was also characterized as function of temperature, with the results plotted in *Figure 5-8*. In this PL, it shows the intensity of the PL decreasing as the temperature increases. The cause of this decrease is also assumed to be the thermally activated exciton disassociation. At the same time, the ratio of the phonon replica peak versus the defect peak increases as the temperature increases. When the temperature is 230K, the defect peak and the phonon replica have nearly the same intensity. This indicates more phonons are allowed in the crystal at high temperature, hence more light has scattered on crystal lattice and generates more phonon-related PL.

We plot the intensity of this defect peak as a function of temperature here in *Figure 5-9* and fit the data to the same activation energy equation. Here we get an approximate activation energy of, Ea=33meV. However, the fit is not quite as good as when fitting the band edge emission, suggesting there are other processes going on at higher temperatures.

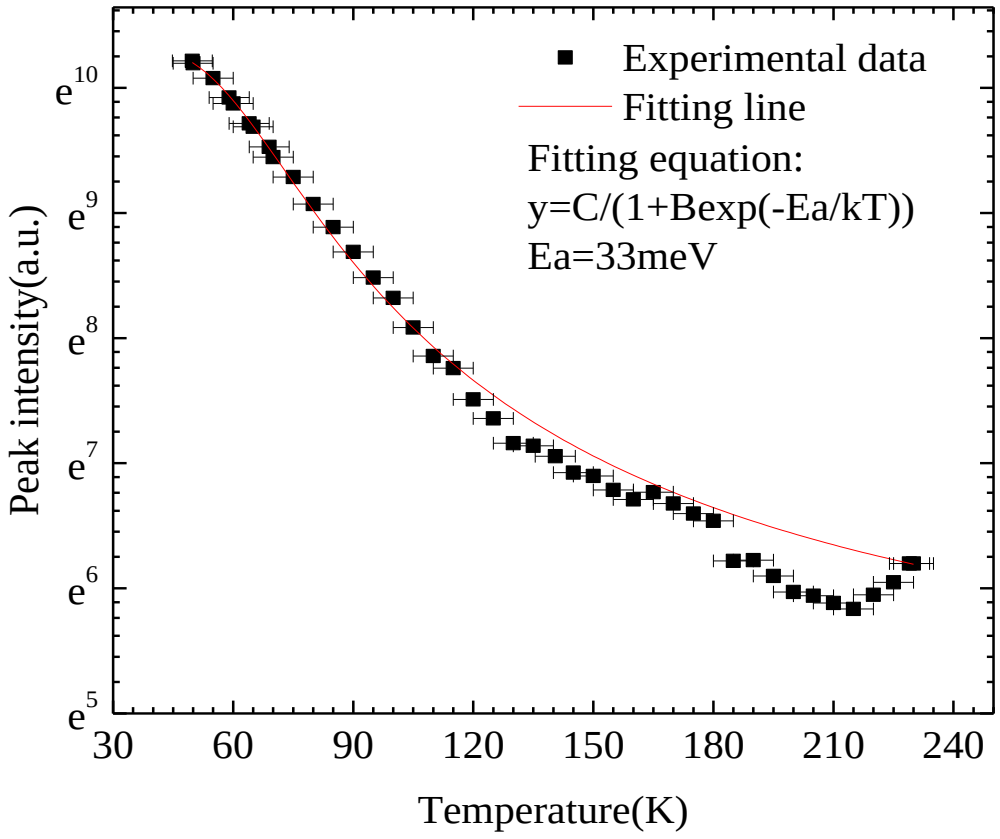

5.2.3 Possible explanation for the defect

From the analysis above, three traits of the PL can be identified. First, this violet fluorescence has a power dependence of 0.68, which means the origin of the fluorescence is a defect related transition [27]. Any free exciton recombination should have a power law

dependence between 1 and 2 [27]. Second, the thermal activation energy of the defect level is 33meV. Which indicated the energy required to dissociate from the level is 33meV. Third, the defect level should be located ~190meV below the conduction band or above the valence band, because the PL peak center is 190meV below the band edge emission PL.

Simply looking at the energy of the defect emissions, there could be three sources of this PL band:

Option1: GaN stacking fault

For low-temperature growth, cubic GaN can spontaneously form and subsequently transition back to hexagonal within individual monolayers [28]. As cubic GaN has a lower band gap, the single layer of cubic GaN acts as a thin quantum well with emission in the range of 3.27eV to 3.48eV [28].

Option2: V_{Ga} single ionized state

The V_{Ga}^{1-} charge state has an energy level at about 0.2eV above the valence band, therefore the transition between the conduction band and V_{Ga}^{1-} level would be emission at 3.29eV.

Option3: Mg doping level and Si doping level

With both Mg doping and Si doping in the material, the expected donor-accepter pair (DAP) recombination between those two levels could have emission at ~3.29eV.

For these samples, option 3 can be ruled out as there is no Mg or Si doping in the GaN growth. Trace amounts are not impossible, but the concentration would be orders of magnitude too low to exhibit a strong emission in between the levels [29]. Option 2 is not

likely as the calculated formation energy of V_{Ga}^{1-} is very high under our growth conditions according to Figure 2-3. Therefore the only reasonable explanation would be option 1. Monolayers of cubic GaN was formed under low-temperature growth conditions of MME.

5.3 Analysis of yellow to red fluorescence band

5.3.1 Emission of deep defect peak

In the long wavelength side of the MME GaN PL spectrum, there is a fluorescence band centered at ~580nm, see *Figure 5-10*. This fluorescence band is very similar to the well-known "yellow band" emission that commonly appears as a defect band in GaN [30]. This has been frequently attributed to the V_{Ga} defect in GaN [30]. In our sample, this band is more significant than is commonly seen in MBE grown GaN [30]. In order to analyze the nature of this emission, the broad PL band was fitted to several peaks. As shown in

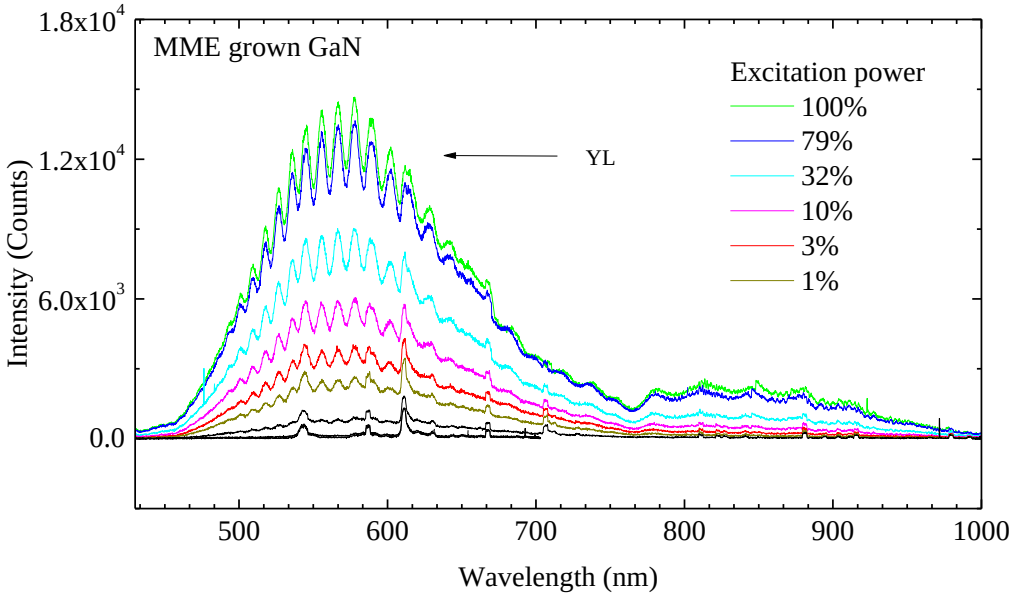

Figure 5-11 a), the broadband can be fitted nicely using three Gaussian peaks. The fringes on top of the broad peak are caused by interference of a 6um thin film, which is the approximate thickness of the template plus the buffer, hence it should be ignored in the fitting. The energy of each peak corresponds to 1.98, 2.22 and 2.42 eV, which is in the middle of the GaN band gap. Therefore, this emission is most likely resulting from the

recombination between band edge and deep defect levels, or the recombination between donor and acceptor pairs (DAP).

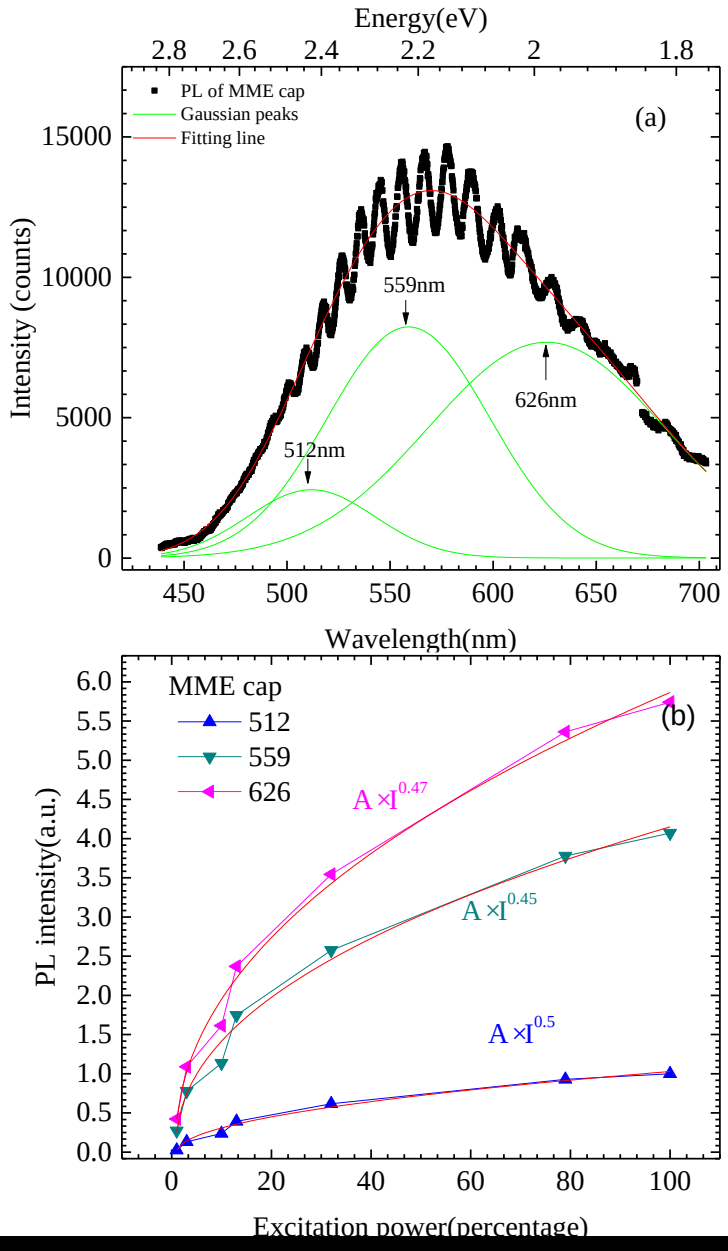

5.3.2 Power dependence measurement of yellow to red band

To further characterize this defect luminescence, we have performed excitation power dependent measurements. In order to reliably keep track of the shape and intensity of this band we can fit each spectrum to three Gaussian peaks as shown in *Figure 5-11 a)*, then track the intensity of each peak as a function of the excitation power. The result shows in *Figure 5-11 b)*, showing that the power dependence of each peak has a power law response with an index between 0.45 and 0.65. This again confirms our expectation that these are defect-related PL [错误!未定义书签。] since they have smaller power law index than band edge emission.

5.3.3Identification of each defect peak

From chapter 2, we have discussed the intrinsic defects that most likely form in GaN. The first principle calculations in Figure 2-3 shows three types of defects that have the lowest formation energy under Ga-rich growth conditions, with a high Fermi level (large electron background concentration). These are V_{Ga}^{3-}, V_N^{3-}, N_i^{1+} and N_i^{1-}. The emission energy of these defect centers could be estimated from the transition energy diagram plotted in Figure 2-4. From Figure 2-4, it was found the recombination of V_{Ga}^{3-} and the band edge would emit at ~2.39eV; the recombination of V_{Ga}^{3-} and the band edge would emit at ~2eV; and the V_N^{3+} is not stable and will therefore not exhibit luminescence. With the above information, it can be concluded that a possible cause of YL should be N_i^{1-} , N_i^{1+} and V_{Ga}^{3-}.

5.4 Conclusion

In this chapter, the luminescence of the MME grown GaN reference sample has been discussed in detail. Specifically, three luminescent bands are found including the band edge emission at 3.484eV, shallow-like defect emission at 3.29eV and deep defect emission at 2.1eV. Each band has been discussed separately. As expected we find the MME growth method did not change the band gap of GaN, however, it did create another significant defect level. The shallow defect emission at 3.29eV suggests a new type of defect that doesn't appear in normal, high-temperature GaN growth. From the temperature-dependent measurement of the 3.29eV peak, we find the activation energy of this violet fluorescence to be 33meV. We tentatively assign this emission band to be the result of cubic GaN stacking faults which form and are in fact enhanced under the low-temperature MME growth conditions. As will be shown below, this defect signal disappears on samples that were grown with In droplets prior to the deposition of the MME cap. The deep defect emission signal can be identified as possibly being from N_i^{1-} and V_{Ga}^{3-} of low formation energy. The most probable candidate for those defect

Chapter 6 In droplet influenced the GaN growth

In the last chapter, we have carefully analyzed the PL spectrum of MME grown low-temperature GaN layer. In this chapter, we will discuss the influence of In droplets on the growth of the MME GaN cap layer. The original purpose to do so is to make InN/GaN droplets and measure their spectrum. However, it turns out In droplets did not crystallized in the MBE chamber. But the PL of the cap layer did change due to the surfactant effect of the In droplets.

6.1 Sample structure.

The sample we used has the following structure:

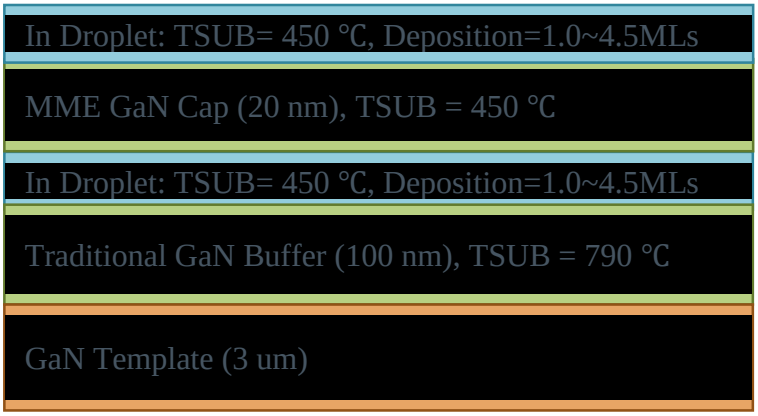

We started the growth of our sample with 3um unintentionally doped GaN templates. Then 100nm GaN buffer layer was deposited on top of the template, with a growth temperature of 790℃. Before the growth of the low temperature MME GaN cap layer, we have deposited In droplets on top of the buffer layer. Activated N plasma was supplied in order to attempt crystallization of the In droplets. Then the MME grown cap layer was deposited on top of the In droplets, with a growth temperature of 450℃. Finally, a similar

layer of In droplets were deposited on the surface for AFM measurements. However, there is no evidence that the droplet crystallized into InN. The In droplet deposition varies from sample to sample, changing from 0ML to 5ML.

6.2 AFM image of In droplet

The surface structure of the sample is shown in Figure 6-2. From the AFM image, we can tell the shape of those In droplet were circular islands, while the crystallized InN droplet should be faceted islands as the strain needs to be released. Therefore the AFM image shows In droplet were not crystallized.

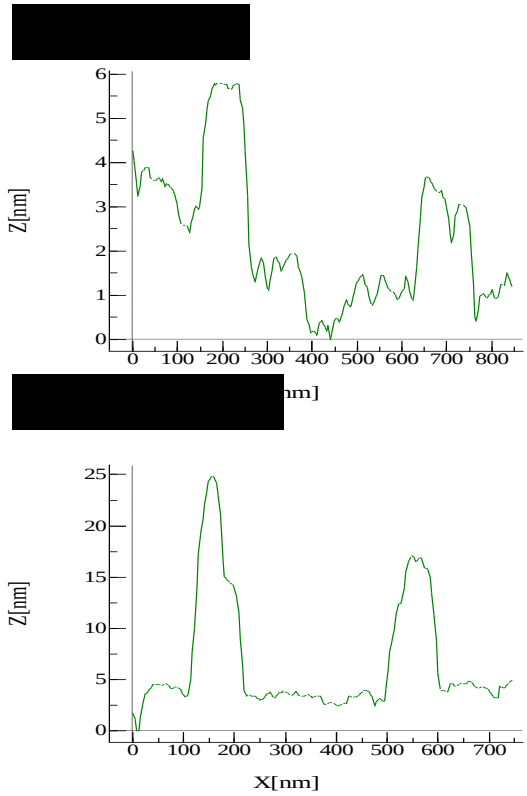

6.3 PL measurement

PL measurements were conducted on this series of the sample with different In depositions. The results are shown in *Figure 6-3*.

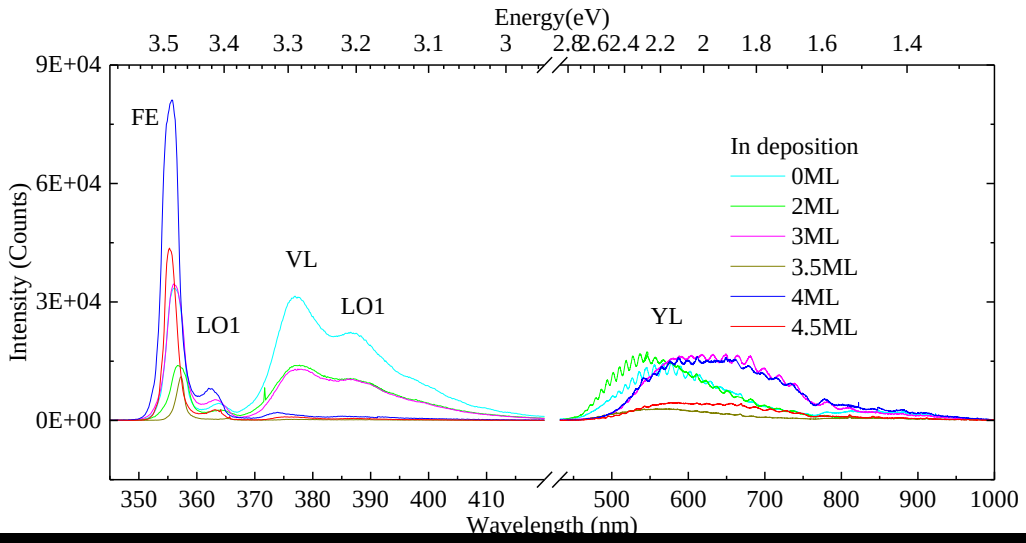

From these spectra, we can see that the ratio of the VL band to the and band edge emission decreases as the In deposition increases. This phenomenon shows the In droplet has influenced the quality of MME grown GaN cap layer, it has stopped the formation of stacking fault which was assumed to be the origin of VL. Relate to the research by Widmann *et al* [31], In has a surfactant effect in GaN growth, therefore we suspect the existence of In droplets has causes the decrease of stacking fault through its surfactant effect.

Then we can look at the PL of 400~800nm range. The PL of each sample shows in *Figure 6-3*. As we can see, the emission in this range was also affected by In droplets. The shape of the PL has varies with In deposition. It indicates the In droplet has a certain effect on

the formation of intrinsic defects that has caused the emission in this range. But the way how it interacts with each other is still not so clear yet.

6.4 Conclusion

In this chapter, we have characterized a series of samples which contain In droplets and MME grown GaN cap layers. From the PL of these samples we can see the VL signal which is emitted from the MME cap layer disappears when more than 3ML of In is deposited before the growth of the MME cap layer. This phenomenon is related to the surfactant effect of In on GaN growth. We can expect this effect also stops the formation of stacking fault which was suspected to be the cause of VL. The PL at 450 to 800nm range, also shows some difference with more In droplet deposition. Which indicates a change of point intrinsic defect formation which have emission at this wavelength. However, there's not a clear pattern how did the In droplet interact with the defect levels.

Chapter 7 Conclusion

In this thesis, we have discussed the optical property of MME grown GaN. In Chapter 4, by comparing the PL signal from the GaN template, GaN template with the 100nm buffer layer, and GaN template with 100nm buffer layer and 20nm MME grown cap layer, we can find MME grown GaN cap layer has suppressed the band edge emission and enhanced the defect related emission. In Chapter 5, through temperature dependence analysis and excitation power dependence analysis of the PL from the MME grown GaN cap layer we can get the following conclusions:

1) The band gap of GaN doesn't change for MME grown GaN. The band gap of GaN is characterized as 3.501±0.014eV. From the thermal quenching of GaN band-edge emission, the dissociation energy of exciton in GaN can be determined as 21meV.

2) A new type of defect with emission at 3.29eV is formed in MME grown GaN. The thermal activation energy of this defect can be determined to be 33meV. The one reasonable explanation of this defect is stacking fault formation from the MME growth. Since the transition energy of stacking fault matches the PL energy we observed.

3) The MME growth method still generates a defect emission between 450nm and 700nm in GaN samples. From the excitation power dependent analysis of those bands, they can be identified as the emission from deep defect levels.

From the optical characterization of MME grown GaN, it is found that the MME grown GaN has quality degradation because a new type of defect was formed, which we strongly suspect to be a stacking fault. In order to make high-quality InN/GaN heterostructures, current growth technique for low-temperature GaN growth needs to be improved. The analysis in this work has diagnosed several types of defect that could have

caused the degradation of GaN crystal quality, which will provide a clue for researchers who intended to develop techniques to improve the quality of low-temperature GaN.

In Chapter 6, we have done the characterization of a series of samples which have In droplet deposition before the growth of MME GaN cap layer. We found the violet fluorescence signal disappears for samples that have more than 3ML In deposition, which indicates the surfactant effect of In droplet has reduced the formation of stacking faults in GaN under MME growth condition.

Reference:

1 W. C. Johnson, J. B. Parson, and M. C. Crew, “Nitrogen compounds of Gallium I. The Ammonites," vol. 326, no. 1924, 1930.

2 H. P. Maruska, “The preparation and properties of vapor-deposited single-crystal-line GaN,” Appl. Phys. Lett., vol. 15, no. 10, p. 327, 1969.

3 S. Yoshida, “Improvements on the electrical and luminescent properties of reactive molecular beam epitaxially grown GaN films by using AlN-coated sapphire substrates," Appl. Phys. Lett., vol. 42, no. 5, p. 427, 1983.

4 H. Search, C. Journals, A. Contact, M. Iopscience, and I. P. Address, “GaN Growth Using GaN Buffer Layer,” Jpn. J. Appl. Phys., vol. 30, pp. L1705–L1707, 1991.

5 H. Search, C. Journals, A. Contact, M. Iopscience, and I. P. Address, “P-Type Conduction in Mg-Doped GaN Treated with Low-Energy Electron Beam Irradiation (LEEBI),” Jpn. J. Appl. Phys., vol. 28, no. 12, pp. L2112–2114, 1989.

6 S. Heikman, S. Keller, S. P. DenBaars, and U. K. Mishra, "Growth of Fe-doped semi-insulating GaN by metalorganic chemical vapor deposition," Appl. Phys. Lett., vol. 81, no. 3, p. 439, 2002.

7 Akasaki, Isamu, Amano, and Hiroshi, "High-efficiency UV and blue emitting devices prepared by MOVPE and low energy electron beam irradiation treatment," Phys. Concepts Mater. Nov. Optoelectron. Device Appl., vol. 1361, p. 138, 1990.

8 L. Overgrown and G. Substrates, “InGaN-Based Blue Light-Emitting Diodes Grown on Epitaxially Laterally Overgrown GaN Substrates InGaN-Based Blue Light-Emitting Diodes Grown on Epitaxially,” jpn. J. Appl. Phys., vol. 37, pp. L839–841, 1998.

9 S. Nakamura, “Present performance of InGaN-based blue/green/yellow LEDs,” Int. Soc. Opt. photonics, vol. 3002, pp. 26–35, Apr. 1997.

10 H. Search, C. Journals, A. Contact, M. Iopscience, and I. P. Address, “InGaN-based violet laser diodes,” Semicond. Sci. Technol., vol. 14, pp. 27–40, 1999.

11 C.-F. Shih, N.-C. Chen, P.-H. Chang, and K.-S. Liu, “Band Offsets of InN/GaN Interface,” Jpn. J. Appl. Phys., vol. 44, no. 11, pp. 7892–7895, Nov. 2005.

12 G. Namkoong, E. Trybus, K. K. Lee, M. Moseley, W. A. Doolittle, and D. C. Look, “Metal modulation epitaxy growth for extremely high hole concentrations above 1019 cm-3 in GaN,” Appl. Phys. Lett., vol. 93, no. 17, p. 172112, 2008.

13 Bougrov V., Levinshtein M.E., Rumyantsev S.L., Zubrilov A., in Properties of Advanced SemiconductorMaterials GaN, AlN, InN, BN, SiC, SiGe . Eds.

14 Y.P. Varshni, “Temperature dependence of the energy gap in semiconductors”, Physica, Volume 34, Issue 1, 1967, Pages 149-154, ISSN 0031-8914.

15 M. A. Reshchikov and H. Morko ç"Luminescence properties of defects in GaN" Journal of Applied Physics Vol. 97, pp. 061301-15 (2005).

16 G. Li, S. J. Chua, S. J. Xu, and W. Wang," Nature and elimination of yellow-band luminescence and donor–acceptor emission of undoped GaN." Appl. Phys. Lett., Vol. 74, no. 19, pp. 2821-2823, May, (1999).

17 B.V. Shanabrook,"LO-phonon-assisted emission edge of free excitons in GaAs and GaAs/Gax Al1-xAs quantum wells", Physical Review B, Vol.41, No.3, pp.41 (1990).

18 E. Shabunina, N. Averkiev, A. Chernyakov, M. Levinshtein, P. Petrov, and N. Shmidt "Extended defect system as the main source of non-radiative recombination in InGaN/GaN LEDs" Phys. Status Solidi. C, Vol 10 No. 3 pp. 335-337, (2013).

19 T. Schmidt and K. Lischka "Excitation power dependence of the near-band-edge photoluminescence of semiconductors" Physical Review B. Vol. 45 no. 16, pp. 45 (1992).

20 A. Y. Cho, J. R. Arthur, "Molecular beam epitaxy". Prog. Solid State Chem. Vol. 10, pp. 157–192, (1975).

21 B. A. Joyce,"Molecular beam epitaxy" Rep. Prog. Phys. Vol. 48 pp. 1639 (1985). Printed in Great Britain,

22 "Molecular Beam Epitaxy." Wikipedia. Wikimedia Foundation, n.d. Web. 18 July 2016.

23 M. A. Reshchikov and H. Morko ç"Luminescence properties of defects in GaN" Journal of Applied Physics Vol. 97, pp. 061301-4 (2005).

24 A. Wysmolek, M. Potemski, R. Stepniewski, J. M. Baranowski, D. C. Look, S. K. Lee, and J. Y. Han, Phys. Status Solidi B Vol. 235, No. 1, pp. 36-39, (2003).

25 J. F. Muth, J. H. Lee, I. K. Shmagin, R. M. Kolbas, H. C. Casey Jr., B. P. Keller, U. K. Mishra, and S. P. DenBaars, “Absorption coefficient, energy gap, exciton binding energy, and recombination lifetime of GaN obtained from transmission measurements” Applied Physics Letters Vol. 71, no. 18, pp. 2572 Nov (1997).

26 W. Shan, B. D. Little, A. J. Fischer, and J. J. Song, “Binding energy for the intrinsic excitons in wurtzite GaN”, Physical Review B, Vol. 54, No. 23, pp. 54, (1994).

27 T. Schmidt* and K. Lischka,"Excitation power dependence of the near-band-edge photoluminescence of semiconductors" Physical Review B, Vol. 45, No. 16, pp.45 (1992).

28 C. Stampfl and Chris G. Van de Walle,"Energetics and electronic structure of stacking faults in AlN, GaN, and InN" Vol. 57, no.24 pp.57 (1998).

29 G. Callsen, M. R. Wagner, T. Kure, J. S. Reparaz, M. Bugler, J. Brunnmeier, C. Nenstiel, and A. Hoffmann, "Optical signature of Mg-doped GaN: Transfer processes" PHYSICAL REVIEW B Vol. 86, 075207 (2012).

30 M. A. Reshchikov, H. Morko ç, S. S. Park, and K. Y. Lee, "Yellow and green luminescence in a freestanding GaN template", Applied physics Letters, Vol. 78, pp. 3041,(2001).

31 F. Widmann, B. Daudin, G. Feuillet, N. Pelekanos, and J. L. Rouvi ère "Improved quality GaN grew by molecular beam epitaxy using In as a surfactant" Applied Physics Letters Vol.73, 2642 (1998).